Supporting Information

Triarylamine-based porous coordination polymers performing both hydrogen atom transfer and photoredox catalysis for regioselective α-amino C(sp^3)–H arylation

Hanning Li, Yang Yang, Xu Jing*, Cheng He and Chunying Duan*

State Key Laboratory of Fine Chemicals, Zhang Dayu College of Chemistry

Dalian University of Technology Dalian, 116024, China

*E-mail: xjing@dlut.edu.cn, cyduan@dlut.edu.cn

Table of Contents:

1. Syntheses and methods

All reagents were used as purchased without further purification. The ligands tricarboxytriphenylamine (H_3**TCA**) and tris(4-(pyridinyl)phenyl)amine (**NPy**$_3$) were synthesized using previously reported procedures[S1,2] and characterized by ^{1}H NMR. Cd-**TCA** was synthesized according to published procedures.[S3]

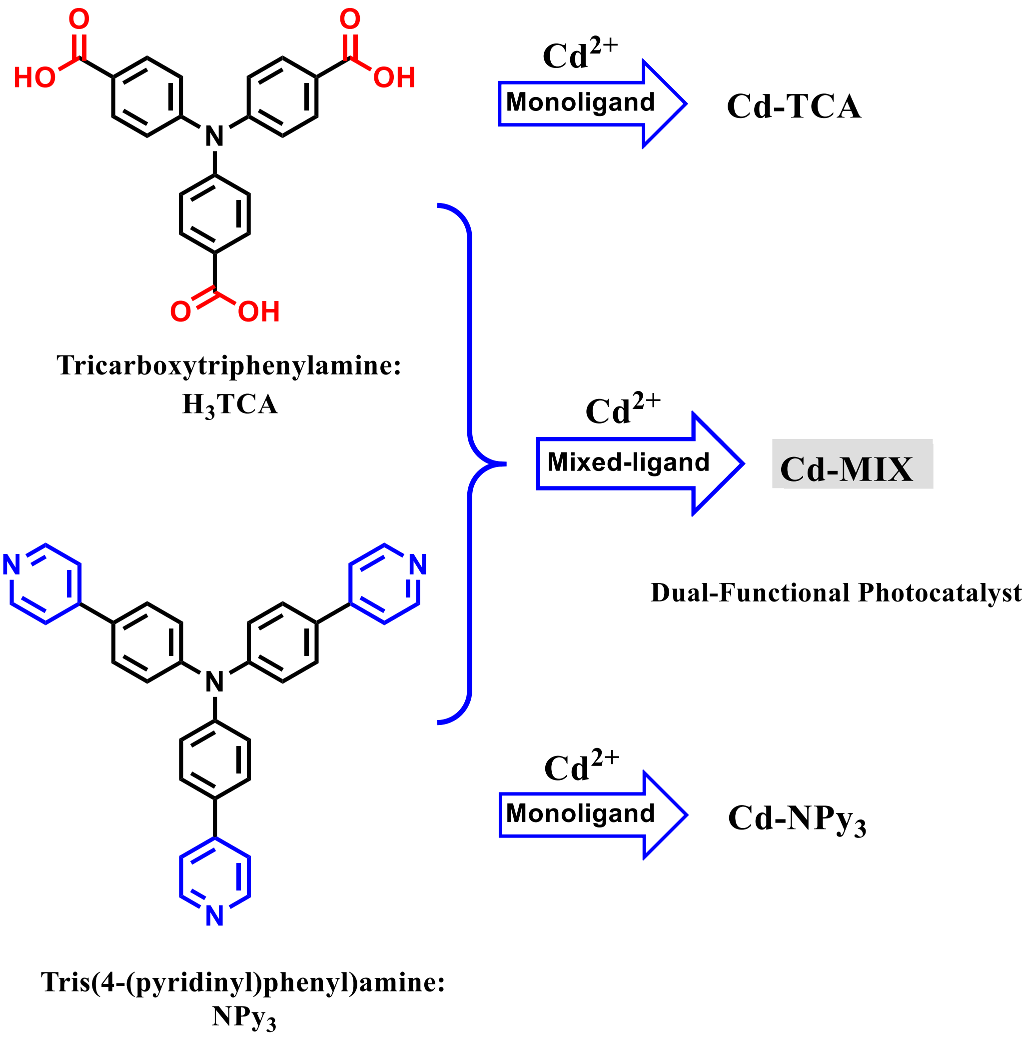

Instruments

Elemental analyses of C, N, and H were performed on a Vario EL III elemental analyzer. Powder X-ray diffraction (PXRD) tests were performed on SmartLab 9kw X-ray diffractometer instrument with a Cu sealed tube. Fourier transform infrared spectroscopy (IR) spectra were recorded using KBr pellets on a JASCO FT/IR-430 instrument. ^{1}H NMR and ^{13}C NMR spectra were recorded on a Varian INOVA 400 M spectrometer. Solution UV−vis spectra were performed on a TU-1900 spectrophotometer. Solid UV−vis spectra were recorded on a Hitachi U-4100 UV−vis−NIR spectrophotometer and a white standard of $BaSO_4$ was used as a reference. Thermogravimetric analyses (TGA) were carried out at a ramp rate of 10 ℃/min up to 800 ℃ under a nitrogen flow with a Mettler-Toledo TGA/SDTA851 instrument.

Scanning electron microscopy (SEM) images were taken using a HITACHI UHR FE-SEM SU8200 microscope. Fluorescent spectra were measured on EDINBURGH F900. GC analyses were performed on an Agilent Technologies 6890 N GC system. Electron paramagnetic resonance (EPR) experiments were measured on Bruker E500 instrument, and the intensity was recorded at 100 K under Ar atmosphere. Cyclic voltammograms (CV) and electrochemical impedance spectroscopy (EIS) plots were measured on ZAHNER ENNIUM electrochemical workstation. Transient photocurrent/time measurements were performed on a CHI 650E electrochemical workstation.

Confocal laser scanning microscopy micrographs were collected by an Olympus Fluoview FV1000 instrument with λ_{ex} = 635 nm. The confocal and bright-field images of the obtained samples were scanned at λ_{em} = 650−750 nm and excited at 635 nm using a 405/488/635 nm filter.

Single crystal X-ray crystallography

Data of Cd-**MIX**, **1a**@Cd-**MIX**, **1c**@Cd-**MIX**, and Cd-**NPy**$_3$ were measured on a Bruker SMART APEX CCD diffractometer with Mo-Kα radiation (λ = 0.71073 Å) using the SMART and SAINT programs.[S4,5] The single crystal structures were solved by direct methods and then refined by full-matrix least-squares refinements on F^2 using the SHELXL-97 software. And an absorption correction was performed using the SADABS program.[S6] The remaining atoms were found from successive full-matrix least-squares refinements on F^2 and Fourier syntheses. Non-H atoms were refined with anisotropic displacement parameters. H atoms in the backbones were fixed geometrically at calculated distances and allowed to ride on the parent non-hydrogen atoms, whereas some of the disordered solvent molecules were not treated during the structural refinements. To help the stability of the refinement for the impregnated related substrate molecules, the bond distances between several atoms were fixed, and thermal parameters on adjacent atoms in two molecules were restrained to be similar. The SQUEEZE program was carried out for crystals Cd-**MIX**, **1a**@Cd-**MIX**, and **1c**@Cd-**MIX**.

Data availability

The X-ray crystallographic coordinates for structures reported in this article have been deposited at the Cambridge Crystallographic Data Centre (CCDC) under the deposition numbers CCDC 1970513, 1970515, 1970516, and 1970538. These data can be obtained free of charge from The Cambridge Crystallographic Data Centre *via* www.ccdc.cam.ac.uk/data_request/cif. All other data supporting the findings of this study are available within the article and its supplementary information files, or from the corresponding author on reasonable request.

The synthesis of *N*-((phenyl-D_5)methyl-D_2)pyrrolidine (1cD)

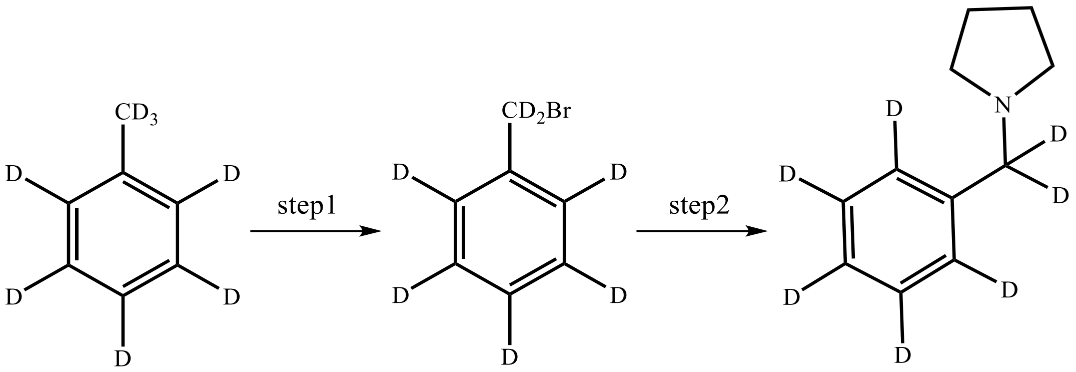

Step1: The [D_7]benzyl bromide was synthesized using previously reported procedures[S7] and characterized by GC-MS. A solution of [D_8]toluene (2.0 g, 20.0 mmol) in CCl_4 (35.0 mL) was added NBS (3.56 g, 20.0 mmol) and benzoyl peroxide (20.0 mg) under nitrogen atmosphere. The mixture was heated at 90 ℃. Upon completion of the reaction (monitored by TLC) the mixture was cooled and filtered then purified by column chromatography to give [D_7]benzyl bromide.

Step2: The *N*-((phenyl-D_5)methyl-D_2)pyrrolidine (**1c**D) was synthesized according to the previously reported procedures[S8] and characterized by ^{1}H NMR, ^{13}C NMR and GC-MS. A solution of [D_7]benzyl bromide (20.0 mmol, 1.0 equiv) in dichloromethane (30.0 mL) was added pyrrolidine (40.0 mmol, 2.0 equiv) and triethylamine (40.0 mmol, 2.0 equiv) at 0 ℃ then warm to room temperature. After stirring 20 h, 1.0 N NaOH solution (40.0 mL) was added to the reaction mixture, and then extracted with DCM. The combined organic layers were dried over $MgSO_4$, filtered, and concentrated under reduced pressure. The crude mixture was purified by column chromatography to afford *N*-((phenyl-D_5)methyl-D_2)pyrrolidine.

Deuterium labeling experiments

The deuterium labeling experiments were carried out by using *N*-((phenyl-D_5)methyl-D_2)pyrrolidine (**1c**D) instead of *N*-benzylpyrrolidine (**1c**) as the coupling partner with 1,4-DCB under optimal conditions. The conversions were determined using ^{1}H NMR. The kinetic isotope effect (KIE) was evaluated by treating *N*-benzylpyrrolidine or *N*-((phenyl-D_5)methyl-D_2)pyrrolidine in two different vessels under optimal conditions, resulting in k_H/k_D as 3.26. Rate constants were obtained *via* kinetic curves of the C–H functionalization reactions using *N*-benzylpyrrolidine or *N*-((phenyl-D_5)-methyl-D_2) pyrrolidine as substrates. Reaction of *N*-benzylpyrrolidine and *N*-((phenyl-D_5)-methyl-D_2)pyrrolidine (mole ratio, 1:1) with 1,4-DCB in one vessel under optimal conditions, resulting in k_H/k_D as 2.78. The result was determined by ^{1}H NMR of the reaction mixture using 1,1,2,2,- tetrachloroethane as internal standard.

Electrochemical measurements

Solid-state cyclic voltammetry (CV) measurements were measured by using a three-electrode system with an Ag/AgCl electrode as a reference electrode, a platinum silk with 0.5 mM diameter as a counter electrode, and a homemade carbon-paste electrode as a working electrode, in a 0.1 M KPF_6 solution at a scan rate of 100 mV s^{-1}. The manufacturing operation of carbon-paste working electrode: a well-ground mixture of sample and carbon paste (graphite and moderate mineral oil) was set in channel of a glass tube and connected to a copper wire. The measurements were performed at room temperature after degassed by nitrogen.

Transient photocurrent/time measurements were performed using standard three-electrode system with the catalyst-coated ITO as the working electrode, an Ag/AgCl as a reference electrode and Pt plate as the counter electrode. A 300 W Xenon lamp was used as light source. A 1.0 M KCl solution was used as electrolyte. The photocatalyst (1.0 mg) was dispersed into a mixed solution with 15.0 μL 5 wt% Nafion, 0.5 mL ethanol, and 0.5 mL H_2O and the working electrodes were prepared by dropping the suspension onto the surface of an ITO plate. The working electrodes were dried, and the photo-responsive signals of the samples were measured under chopped light with a bias potential of –0.01 V.

Electrochemical impedance spectroscopy (EIS) measurements were measured using a three-electrode system with the photocatalyst-coated glassy carbon as the working electrode, Pt silk as counter electrode, and an Ag/AgCl as a reference electrode. A 1.0 M KCl aqueous solution was used as the electrolyte. The photocatalyst (1.0 mg) was dispersed into 15.0 μL 5 wt% Nafion, 0.5 mL ethanol, and 0.5 mL H_2O mixed solution, and the working electrode was prepared by dropping the suspension onto the surface of the glassy carbon electrode. The working electrode was dried, and then EIS measurements were performed with a bias potential of –1.40 V for Cd-based coordination polymers in the dark.

Table S1. Crystal data and structure refinements

Entry	Cd-**MIX**	**1a**@Cd-**MIX**	**1c**@Cd-**MIX**	Cd-**NPy$_3$**
Empirical formula	$C_{78}H_{57}Cd_3N_7O_{15}$	$C_{84}H_{66}Cd_3N_{7.50}O_{18}$	$C_{84}H_{64.50}Cd_3N_{7.50}O_{15}$	$C_{72}H_{66}CdCl_2N_{10}O_4$
Formula weight	1669.50	1805.64	1756.13	1318.64
Crystal system	Monoclinic	Monoclinic	Monoclinic	Monoclinic
Space group	C2/c	C2/c	C2/c	P 2_1/c
a, Å	37.221(2)	37.209(2)	37.379(2)	14.5574(11)
b, Å	26.9129(16)	26.8586(16)	26.8868(14)	18.5530(14)
c, Å	22.3987(14)	22.6033(14)	22.4538(12)	11.8054(9)
α, °	90	90	90	90
β, °	111.130(1)	111.558(1)	111.4061(11)	90.090(1)
γ, °	90	90	90	90
V, Å^3	20929(2)	21009(2)	21009.2(19)	3188.4(4)
Z	8	8	8	2
D_{calcd}, g cm^{-3}	1.060	1.142	1.110	1.374
T, K	200(2)	200(2)	200(2)	200(2)
Rflns	59446	61332	80511	36093
unique rflns	17978	18419	24261	5602
R_{int}	0.0488	0.0405	0.0592	0.0355
μ, mm^{-1}	0.654	0.658	0.654	0.485
GOF	1.145	1.109	1.046	1.026
F(000)	6704.0	7284.0	7080.0	1364.0
$R_1{}^a$ ($I > 2\sigma$)	0.0539	0.0795	0.0639	0.0294
$wR_2{}^b$ (all data)	0.1560	0.2636	0.2335	0.0829
Largest diff. peak and hole (e. Å^{-3})	1.090/ -0.808	3.056/ -1.858	2.754/ -0.931	0.585/ -0.518
CCDC	1970538	1970513	1970515	1970516

^{a} $R_1 = \sum||F_o| - |F_c||/\sum|F_o|$. ^{b} $wR_2 = \sum[w(F_o{}^2 - F_c{}^2)^2]/\sum[w(F_o{}^2)^2]^{1/2}$

Table S2. Part data of the bond length and bond angle of Cd-**MIX**

Bond	Length (Å)	Bond	Length (Å)
Cd(1)–O(17)#7	2.273(3)	Cd(2)–O(6)	2.375(3)
Cd(1)–O(3)	2.271(4)	Cd(2)–O(4)	2.478(3)
Cd(1)–O(18)	2.290(3)	Cd(2)–O(7)#4	2.605(3)
Cd(1)–N(1)	2.305(4)	Cd(3)–O(8)	2.244(4)
Cd(1)–O(7)#1	2.320(3)	Cd(3)–N(4)#9	2.290(5)
Cd(1)–O(19)	2.448(3)	Cd(3)–O(21A)#2	2.273(4)
Cd(2)–O(5)	2.262(3)	Cd(3)–O(11)	2.298(4)
Cd(2)–N(3)#8	2.262(4)	Cd(3)–O(20A)#2	2.352(4)
Cd(2)–O(12)#3	2.313(4)	Cd(3)–O(9)	2.414(4)
Cd(2)–O(6)#4	2.343(3)		

Bond	Angle (°)	Bond	Angle (°)
O(17)#7–Cd(1)–O(3)	87.04(15)	N(3)#8–Cd(2)–O(4)	84.55(12)
O(17)#7–Cd(1)–O(18)	150.49(13)	O(12)#3–Cd(2)–O(4)	88.05(12)
O(3)–Cd(1)–O(18)	88.97(14)	O(6)#4–Cd(2)–O(4)	172.42(11)
O(17)#7–Cd(1)–N(1)	92.52(15)	O(6)–Cd(2)–O(4)	98.77(11)
O(3)–Cd(1)–N(1)	173.63(14)	O(5)–Cd(2)–O(7)#4	81.84(10)
O(18)–Cd(1)–N(1)	94.50(13)	N(3)#8–Cd(2)–O(7)#4	135.99(12)
O(17)#7–Cd(1)–O(7)#1	111.84(12)	O(12)#3–Cd(2)–O(7)#4	77.49(11)
O(3)–Cd(1)–O(7)#1	85.08(13)	O(6)#4–Cd(2)–O(7)#4	52.39(10)
O(18)–Cd(1)–O(7)#1	96.90(12)	O(6)–Cd(2)–O(7)#4	97.29(10)
N(1)–Cd(1)–O(7)#1	89.20(13)	O(4)–Cd(2)–O(7)#4	135.04(10)
O(17)#7–Cd(1)–O(19)	95.23(13)	O(8)–Cd(3)–N(4)#9	120.81(16)
O(3)–Cd(1)–O(19)	87.30(13)	O(8)–Cd(3)–O(21A)#2	104.29(17)
O(18)–Cd(1)–O(19)	55.36(12)	N(4)#9–Cd(3)–O(21A)#2	134.57(18)
N(1)–Cd(1)–O(19)	99.07(14)	O(8)–Cd(3)–O(11)	93.43(16)
O(7)#1–Cd(1)–O(19)	151.38(11)	N(4)#9–Cd(3)–O(11)	90.99(18)
O(5)–Cd(2)–N(3)#8	139.60(12)	O(21A)#2–Cd(3)–O(11)	80.58(18)
O(5)–Cd(2)–O(12)#3	88.52(13)	O(8)–Cd(3)–O(20A)#2	144.80(18)
N(3)#8–Cd(2)–O(12)#3	87.72(14)	N(4)#9–Cd(3)–O(20A)#2	87.24(18)
O(5)–Cd(2)–O(6)#4	131.22(11)	O(21A)#2–Cd(3)–O(20A)#2	54.47(17)
N(3)#8–Cd(2)–O(6)#4	89.17(12)	O(11)–Cd(3)–O(20A)#2	107.95(18)
O(12)#3–Cd(2)–O(6)#4	95.97(12)	O(8)–Cd(3)–O(9)	55.45(15)
O(5)–Cd(2)–O(6)	95.12(12)	N(4)#9–Cd(3)–O(9)	88.27(17)
N(3)#8–Cd(2)–O(6)	93.19(13)	O(21A)–Cd(3)–O(9)	124.77(18)
O(12)#3–Cd(2)–O(6)	173.18(11)	O(11)–Cd(3)–O(9)	141.85(15)
O(6)#4–Cd(2)–O(6)	77.30(12)	O(20A)–Cd(3)–O(9)	110.11(18)
O(5)–Cd(2)–O(4)	55.12(11)		

#1 –x, –y+1, –z+2; #2 –x+1/2, y–1/2, –z+5/2; #3 –x+1/2, –y+1/2, –z+2; #4 –x, y, –z+3/2; #7 –x+1/2, y+1/2, –z+5/2; #8 –x, y–1, –z+3/2; #9 x+1/2, y–1/2, z+1.

Table S3. Part data of the bond length and bond angle of Cd-**NPy$_3$**

Bond	Length (Å)	Bond	Length (Å)
Cd(1)–N(1)	2.3819(16)	Cd(1)–N(2)#1	2.4180(16)
Cd(1)–N(1)#1	2.3819(16)	Cd(1)–Cl(1)	2.5919(5)
Cd(1)–N(2)	2.4180(16)	Cd(1)–Cl(1)#1	2.5919(5)
Bond	**Angle (°)**	**Bond**	**Angle (°)**
N(1)–Cd(1)–N(1)#1	180.0	N(2)–Cd(1)–Cl(1)	90.05(4)
N(1)–Cd(1)–N(2)	87.45(6)	N(2)#1–Cd(1)–Cl(1)	89.95(4)
N(1)#1–Cd(1)–N(2)	92.55(6)	N(1)–Cd(1)–Cl(1)#1	90.93(4)
N(1)–Cd(1)–N(2)#1	92.55(6)	N(1)#1–Cd(1)–Cl(1)#1	89.06(4)
N(1)#1–Cd(1)–N(2)#1	87.45(6)	N(2)–Cd(1)–Cl(1)#1	89.95(4)
N(2)–Cd(1)–N(2)#1	180.0	N(2)#1–Cd(1)–Cl(1)#1	90.05(4)
N(1)–Cd(1)–Cl(1)	89.07(4)	Cl(1)–Cd(1)–Cl(1)#1	180.0
N(1)#1–Cd(1)–Cl(1)	90.94(4)		

#1 –x+1, –y, –z+2.

2. Supplementary structural figures

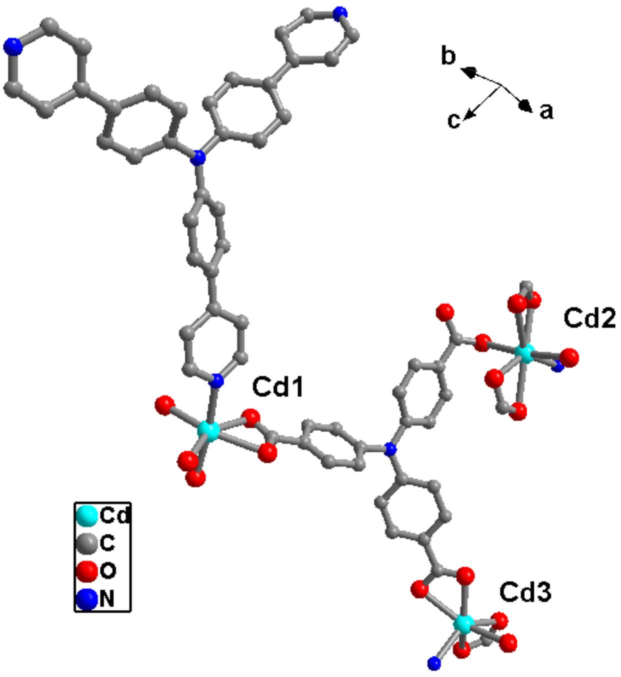

Figure S1. The coordinated environment of three Cd ions in Cd-**MIX**.

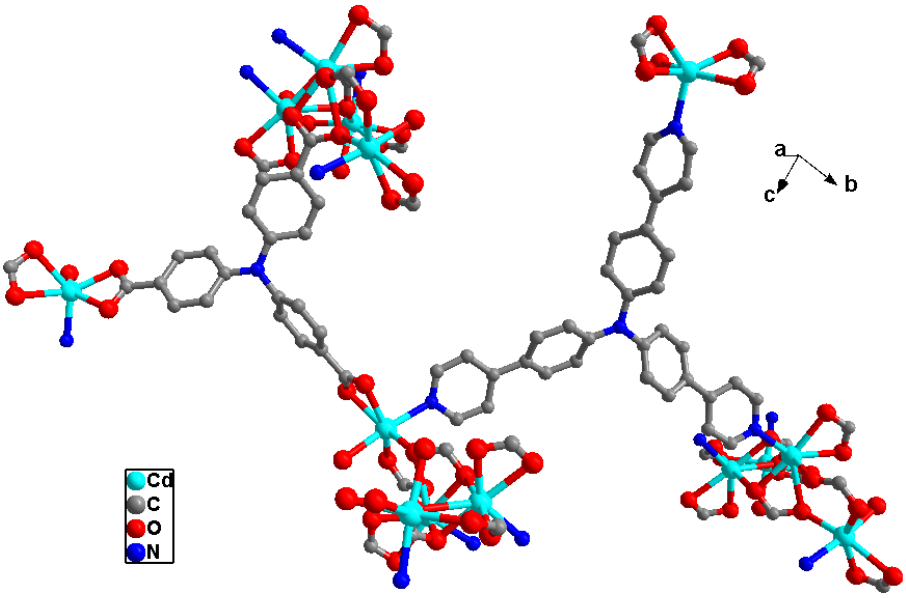

Figure S2. The coordinated environment of **TCA**$^{3-}$ and **NPy**$_3$ in Cd-**MIX**.

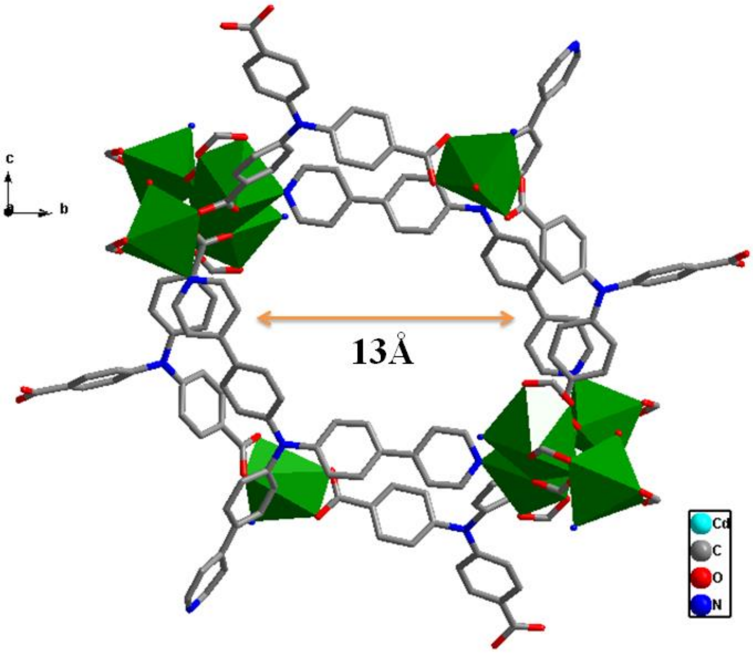

Figure S3. The 8.6 ×13.0 Å^2 open channel of the Cd-**MIX**.

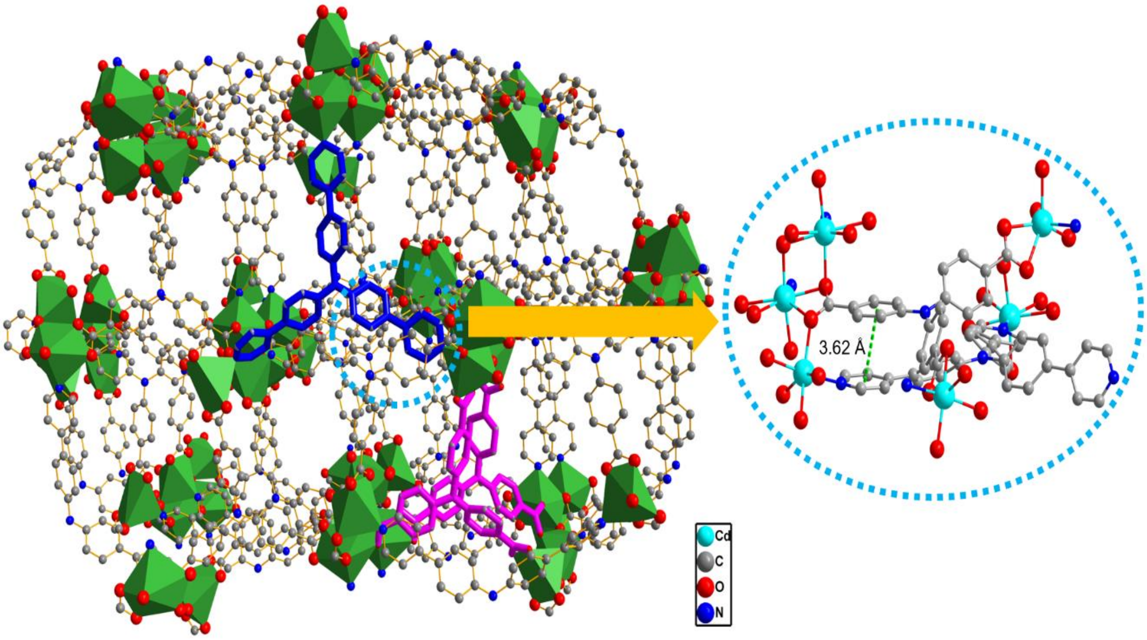

Figure S4. The ball-and-stick representation of H$_3$**TCA** and **NPy$_3$** fragments in Cd-**MIX**.

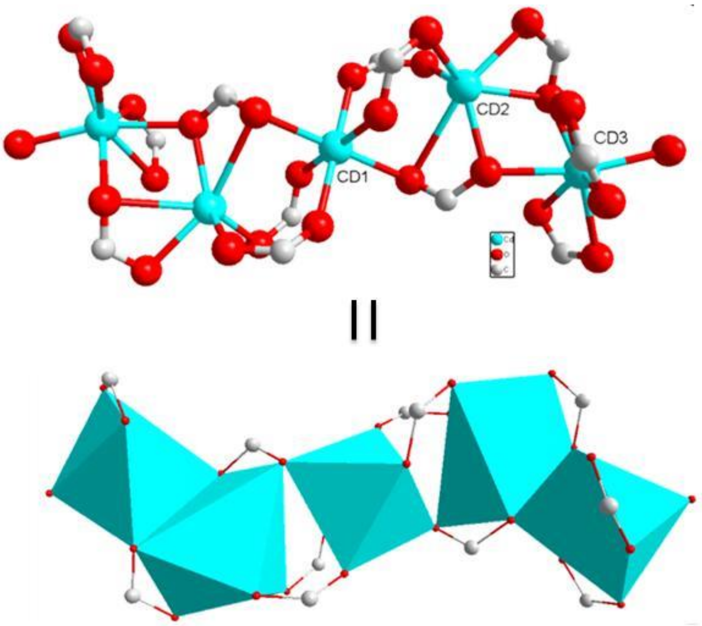

Figure S5. The structure of pentanuclear Cd cluster in Cd-**TCA**.

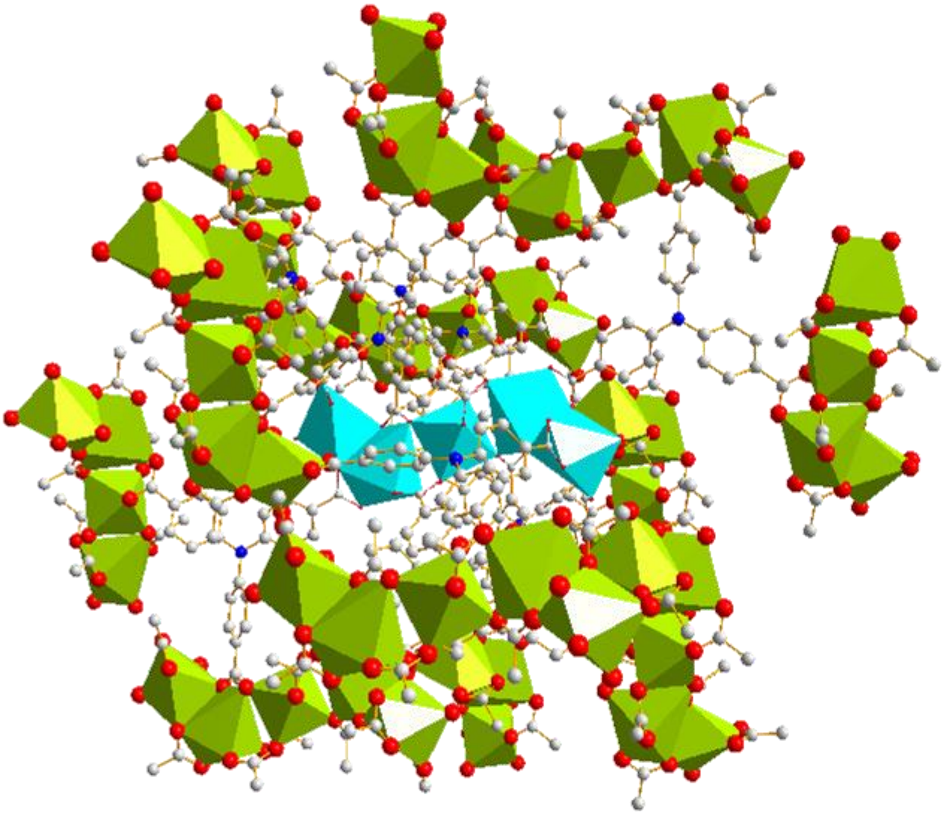

Figure S6. A pentanuclear Cd (II) cluster as a 12-connected node in Cd-**TCA**.

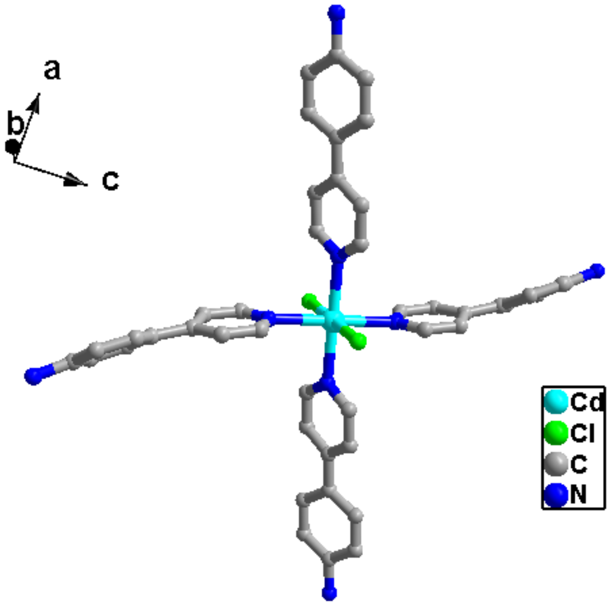

Figure S7. The coordinated environment of Cd (II) ion in Cd-**NPy$_3$**.

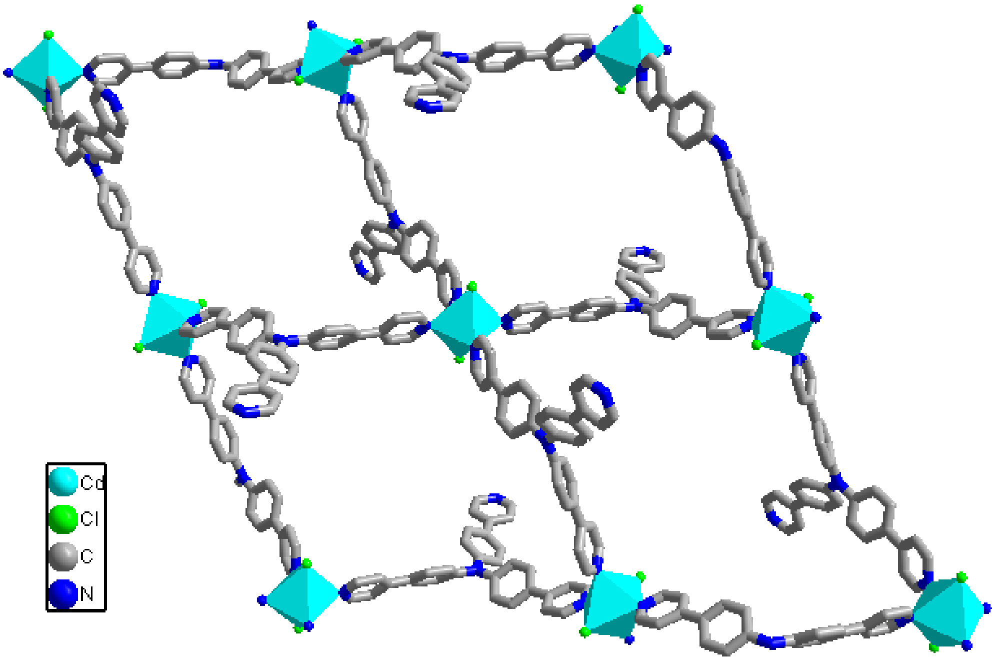

Figure S8. The stick representation of **NPy$_3$** fragments in Cd-**NPy$_3$**.

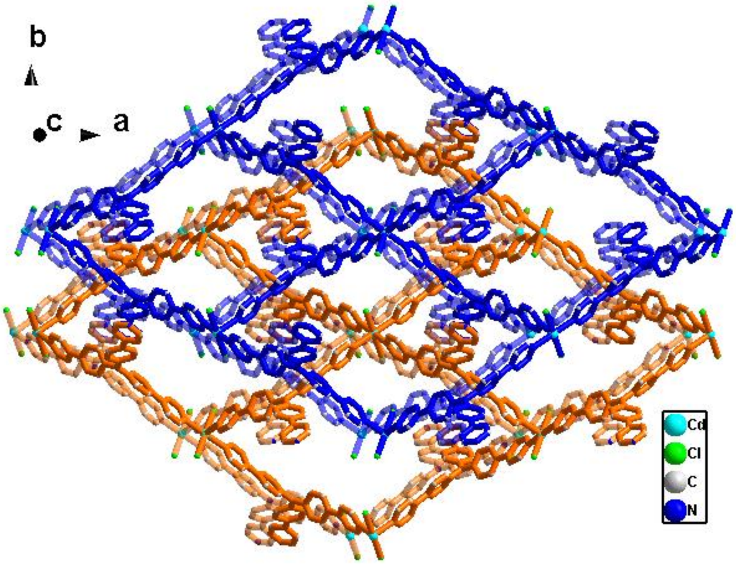

Figure S9. View of the multilayer structure stacked parallelly in an ABAB mode in Cd-**NPy₃**.

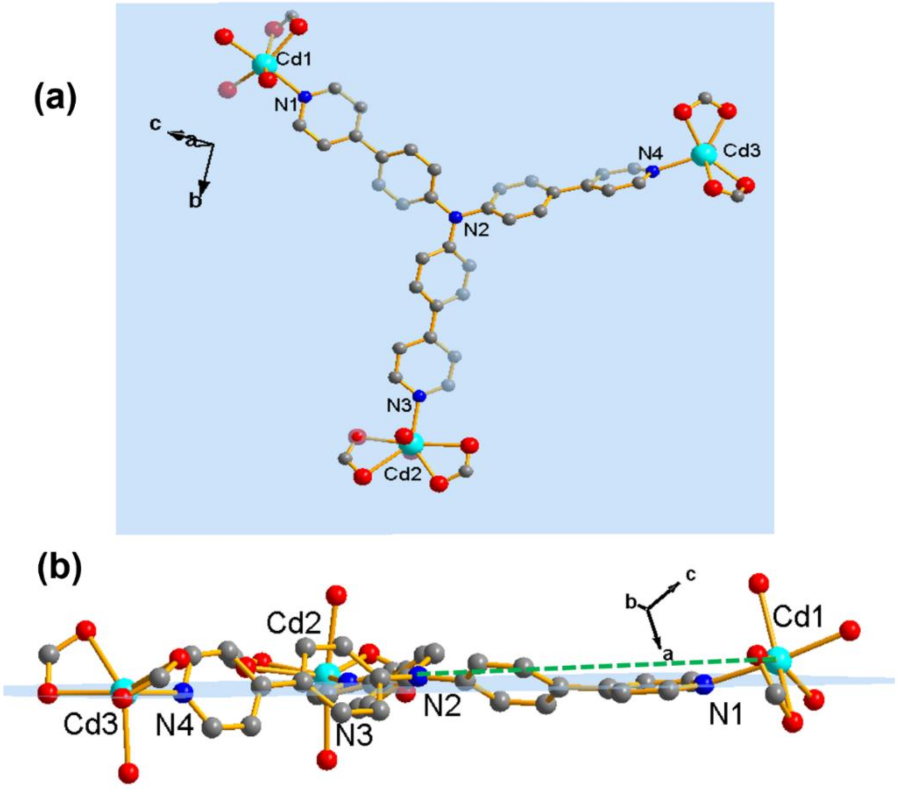

Figure S10. Planar and lateral views of the three N coordination sites of the **NPy₃** in Cd-**MIX**.

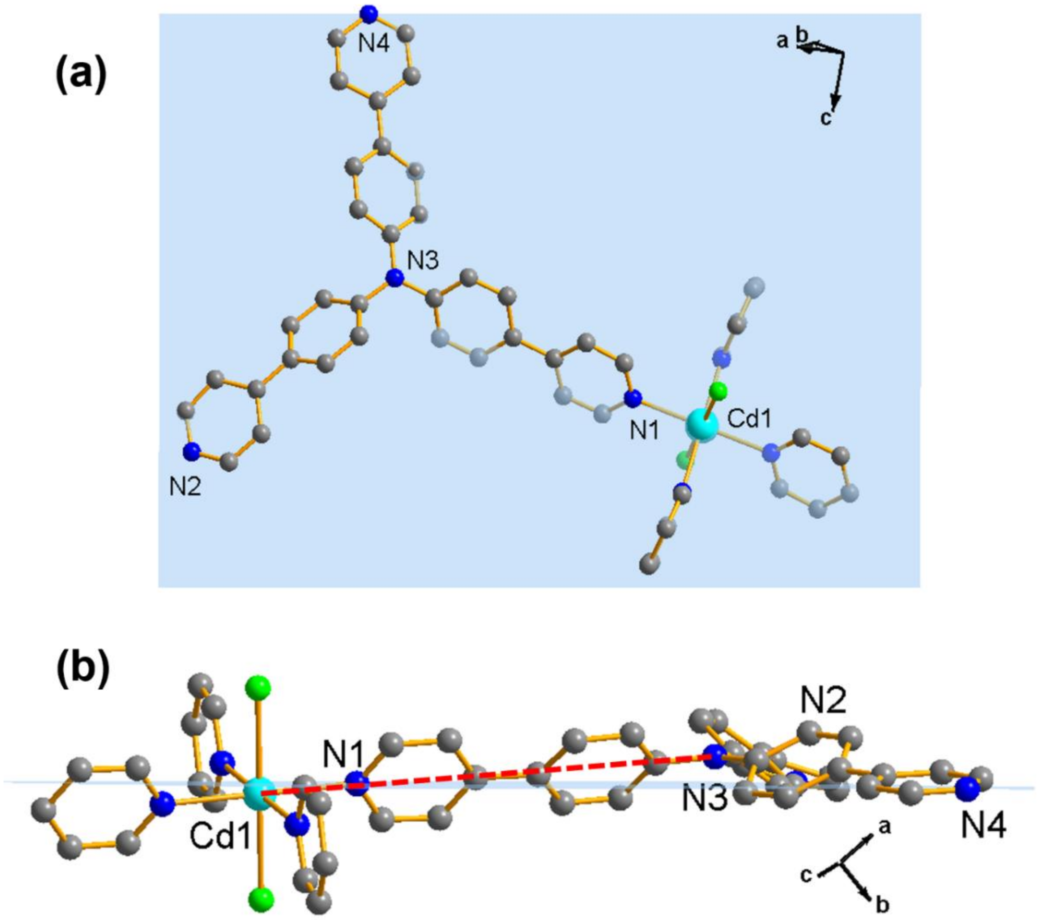

Figure S11. Planar and lateral views of the three N coordination sites of the **NPy$_3$** in Cd-**NPy$_3$**.

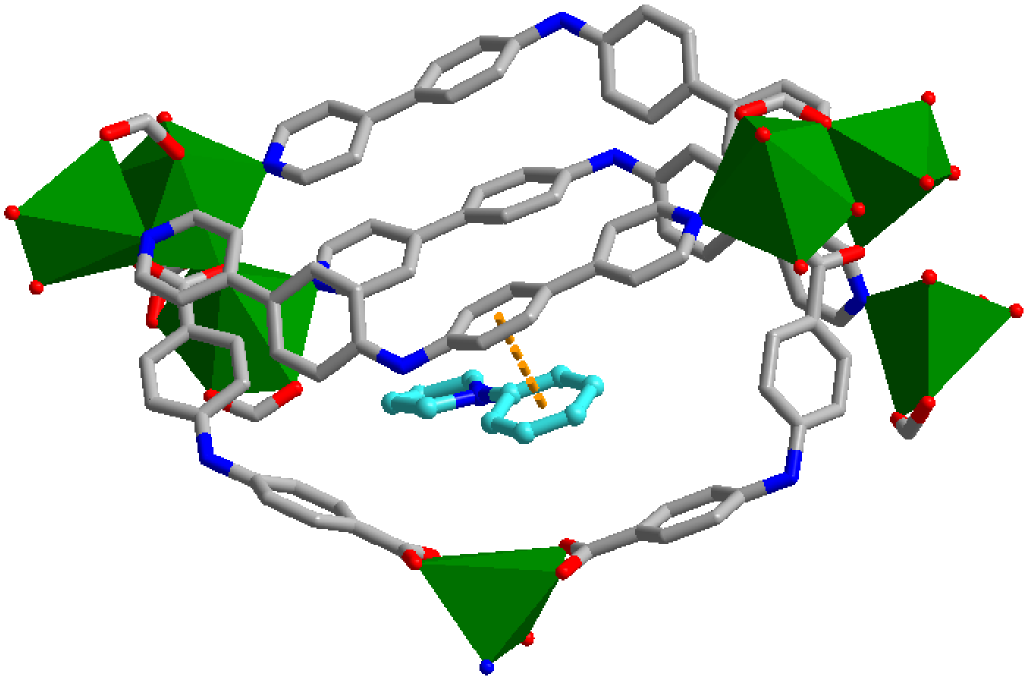

Figure S12. Crystal structures of Cd-**MIX** absorbed substrate **1a**.

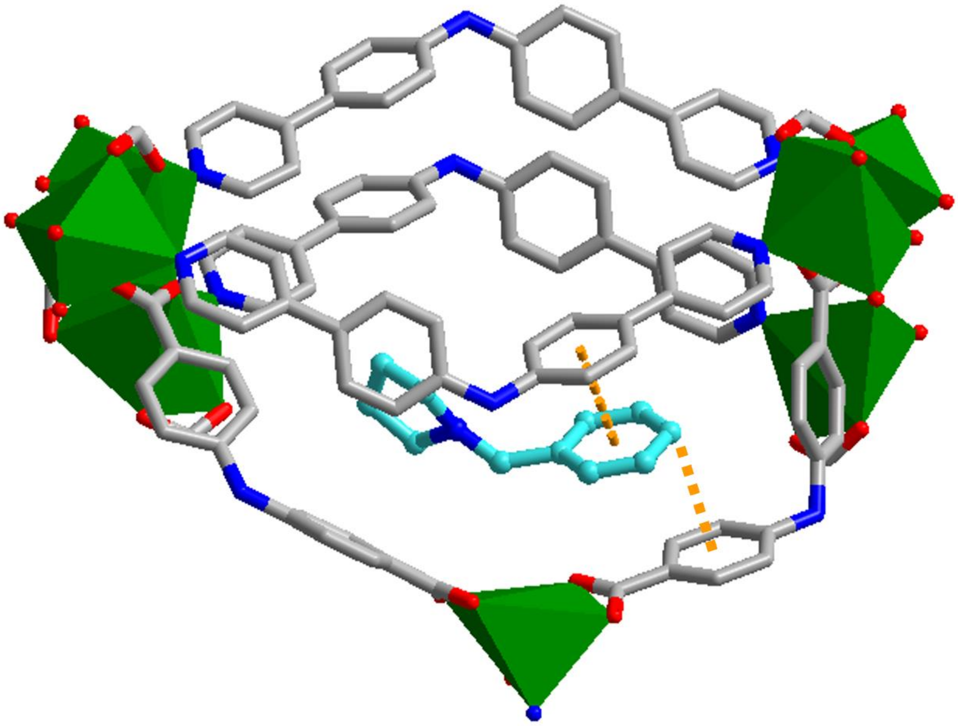

Figure S13. Crystal structures of Cd-**MIX** absorbed substrate **1c**.

3. Characterizations of catalysts

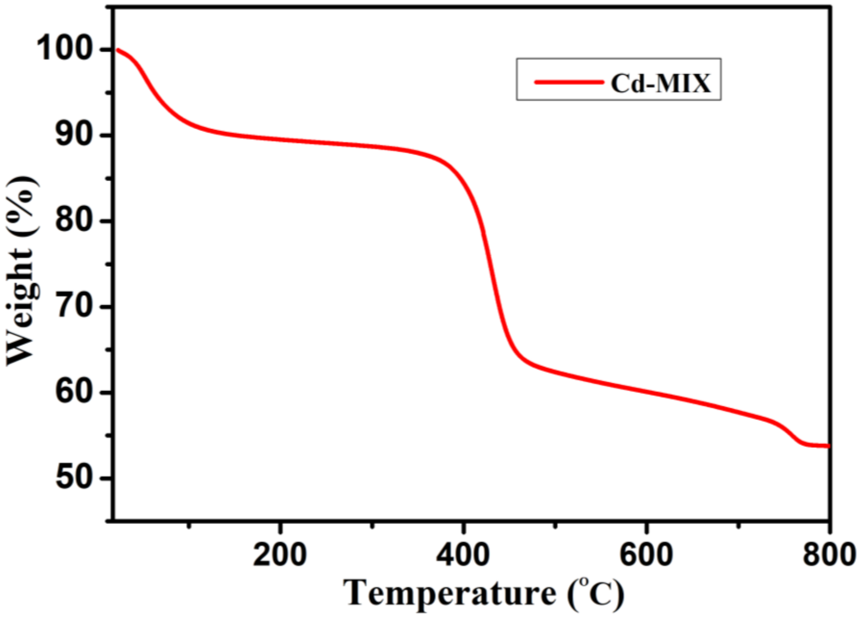

Figure S14. Thermogravimetric (TGA) figure of the prepared Cd-**MIX**.

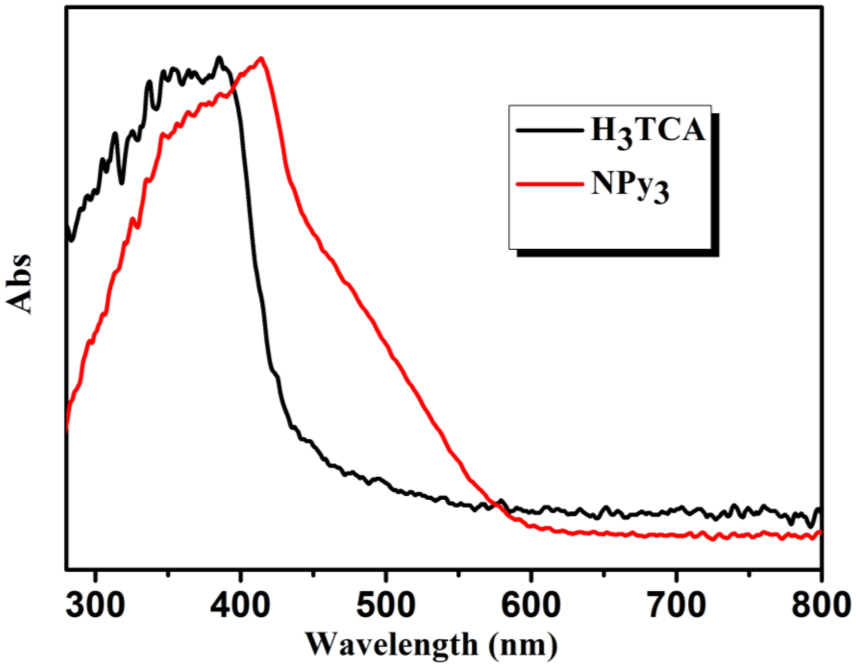

Figure S15. Solid state UV-vis absorption spectra of ligands H_3**TCA** and **NPy$_3$**.

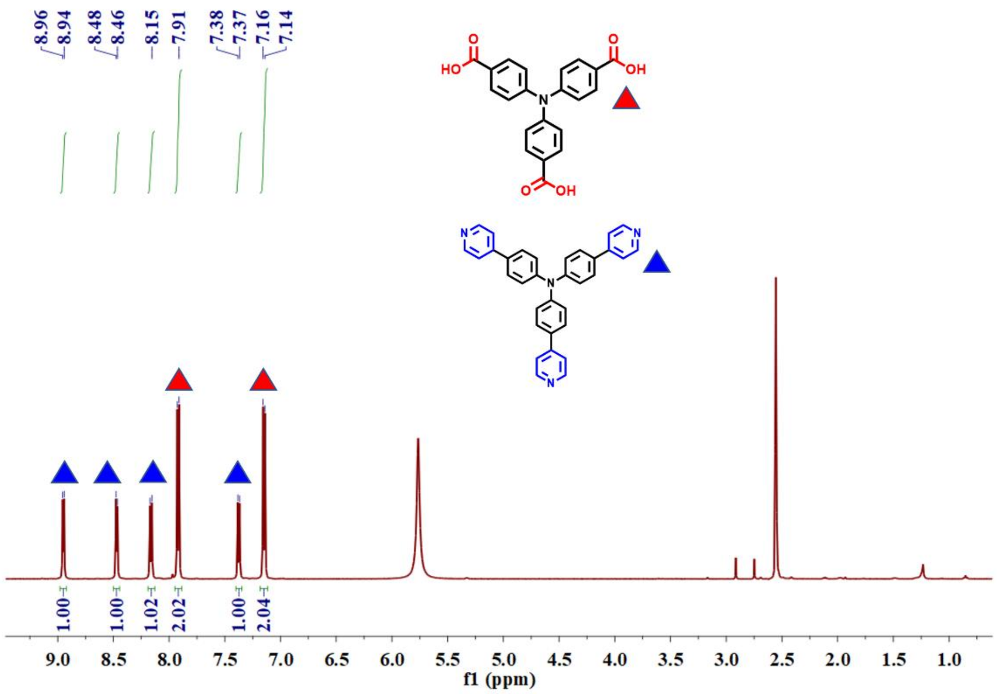

Figure S16. ^{1}H NMR of Cd-**MIX** in DMSO-d_6/DCl giving a 2:1 mole ratio of **TCA**$^{3-}$ ligand and **NPy$_3$** ligand.

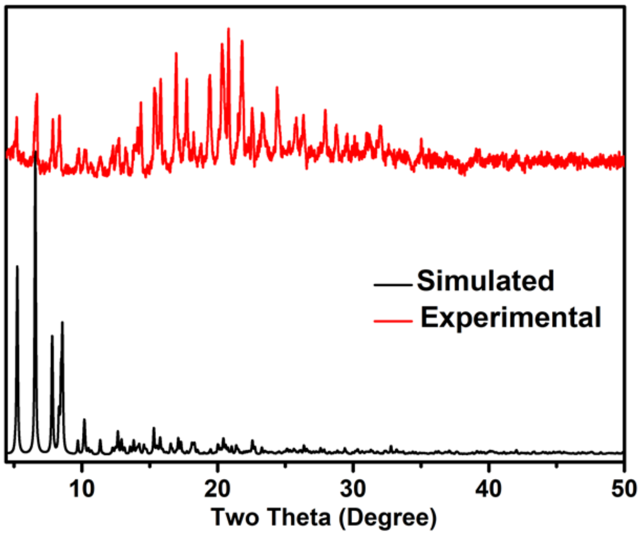

Figure S17. PXRD patterns of Cd-**MIX** showing the calculated pattern based on the single-crystal (black) and as-synthesized Cd-**MIX** (red).

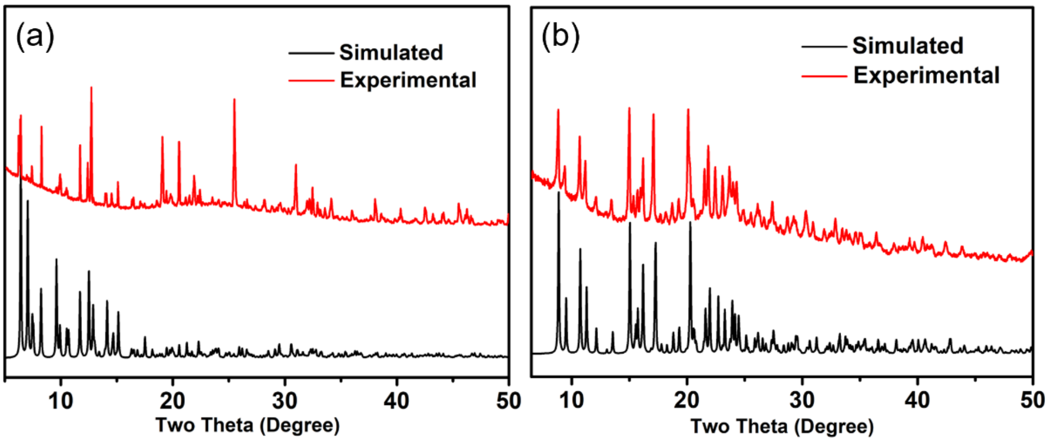

Figure S18. PXRD patterns of Cd-**TCA** (a) and Cd-**NPy**$_3$ (b) showing the calculated patterns based on the single-crystal (black) and as-synthesized samples (red).

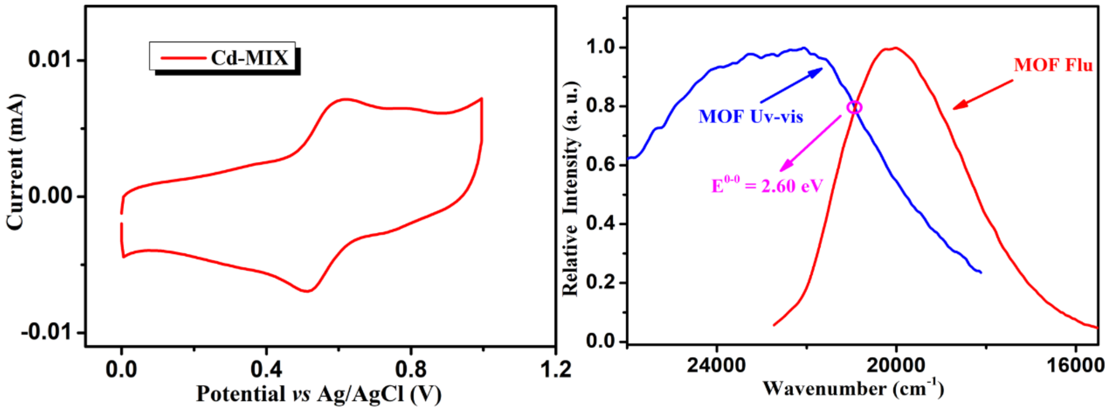

Figure S19. (Left) Solid-state cyclic voltammogram of Cd-**MIX** with a scan rate of 100 mV s^{-1}. (Right) Normalized absorption (blue line) and emission (red line) spectra of Cd-**MIX**.

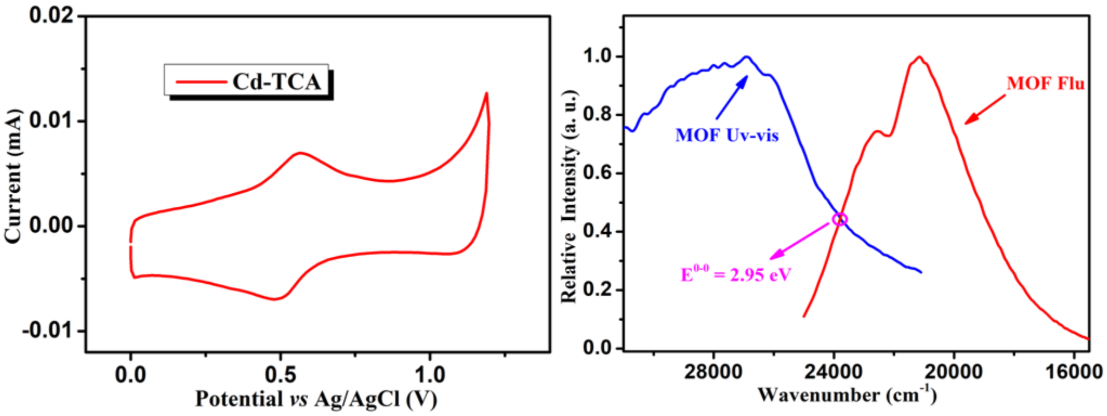

Figure S20. (Left) Solid-state cyclic voltammogram of Cd-**TCA** with a scan rate of 100 mV s^{-1}. (Right) Normalized absorption (blue line) and emission (red line) spectra of Cd-**TCA**.

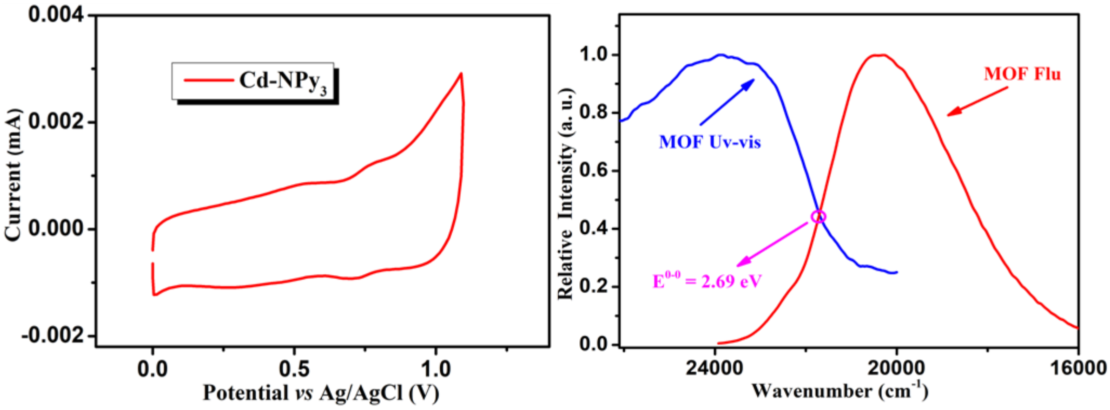

Figure S21. (Left) Solid-state cyclic voltammogram of Cd-**NPy$_3$** with a scan rate of 100 mV s^{-1}. (Right) Normalized absorption (blue line) and emission (red line) spectra of Cd-**NPy$_3$**.

Specific experimental process for dye uptake and confocal laser scanning microscopy of Cd-MIX

Dye uptake. Firstly, Cd-**MIX** was soaked in methanol solution (48 h) for small molecules exchange before the adsorption of dye, and then fully dried out the small molecules in a vacuum oven (100 ℃, 10 h). Then, the crystals Cd-**MIX** were soaked in a 24.0 mM methanol solution of methylene blue dye (2.0 mL), and put the vessels on a constant temperature oscillation incubator for 12 h. The resulting crystals were filtered and washed with fresh methanol rapidly till the solution become colorless to thoroughly remove all the dye attached to the surface of the crystal, and then dried under ambient temperature. The dried samples were dissociated using concentrated hydrochloric acid after dried under the air at room temperature. And the mixed clear solution was diluted to 25.0 mL and adjusted the pH to 0.2. The UV-vis spectrum of the above solution was performed on a UV-vis spectrophotometer. The resulting dye adsorption amount was determined by comparing the UV-vis absorption with a standard curve.

Confocal laser scanning microscopy. The crystals of Cd-**MIX** were soaked in a methanol solution of methylene blue and handled in the same way with the experiments of dye uptake mentioned above. The brightfield and confocal images of the processed samples were scanned at λ_{em} = 650–750 nm, exited by 635 nm through a 405/488/635 nm filter.

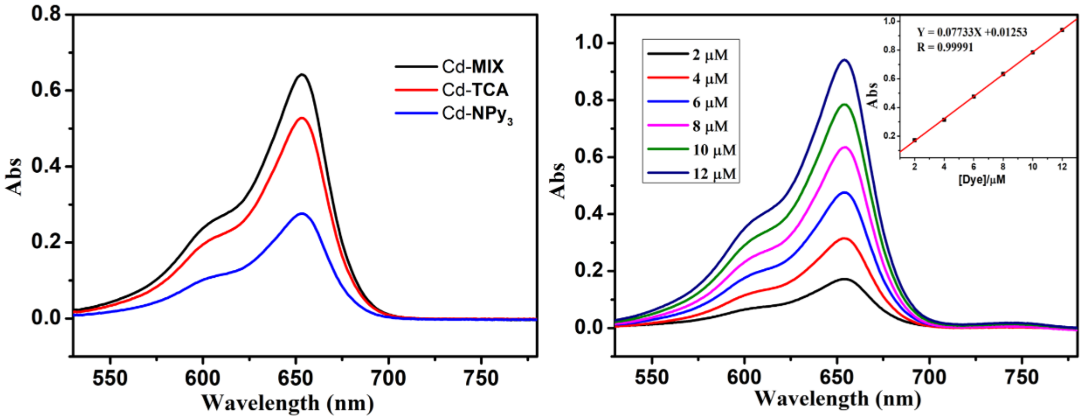

Figure S22. (Left) UV-vis measurement of methylene blue dye released from Cd-**MIX**. (Right) UV-vis measurement of different concentration of methylene blue dye; inside: The standard linear relationship between the absorption and the concentration of methylene blue dye.

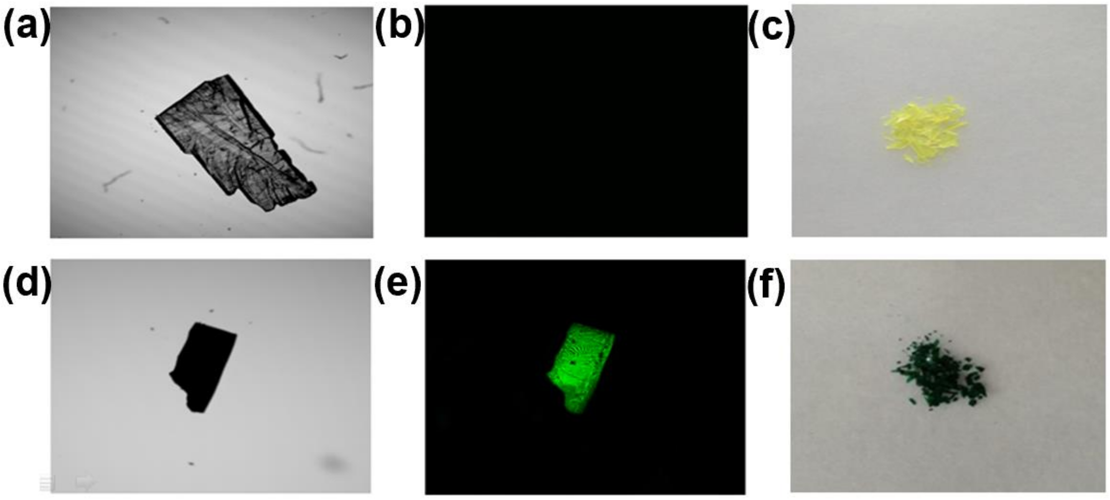

Figure S23. Confocal images of empty (Top) and soaked (Bottom) methylene blue dye. Brightfield images (a,d) and confocal images (b,e) detected at λ_{em} = 650–750 nm, exited by 635 nm through a 405/488/635 nm filter.

4. Host-guest properties between polymers and substrates

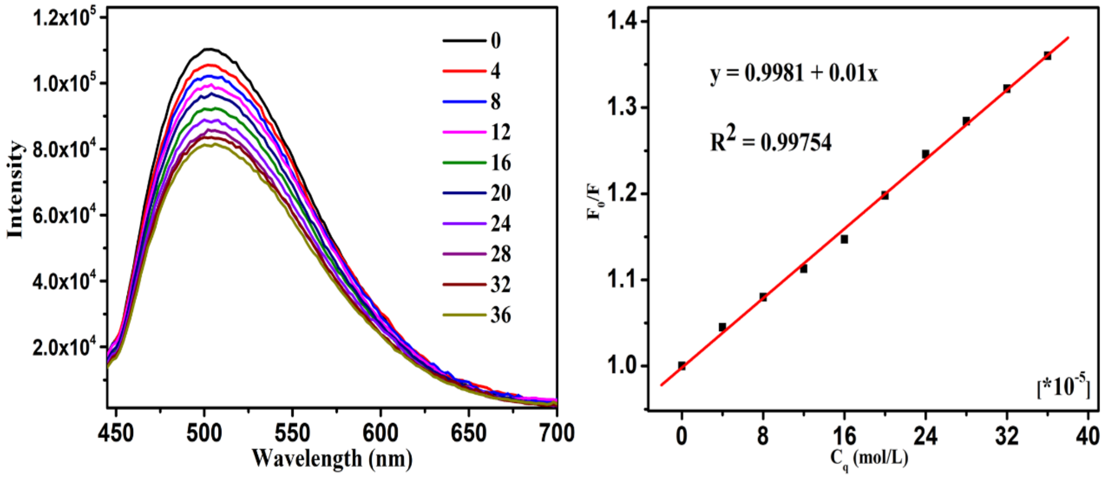

Figure S24. Fluorescence quenching spectra of Cd-**MIX** upon the addition of 1,4-dicyanobenzene and the corresponding simulated Stern-Volmer curve.

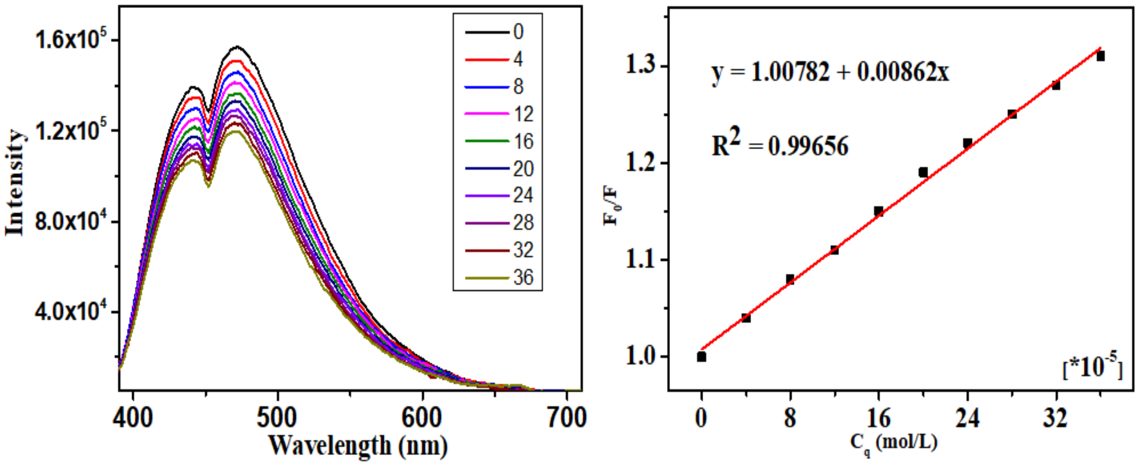

Figure S25. Fluorescence quenching spectra of Cd-**TCA** upon the addition of 1,4-dicyanobenzene and the corresponding simulated Stern-Volmer curve.

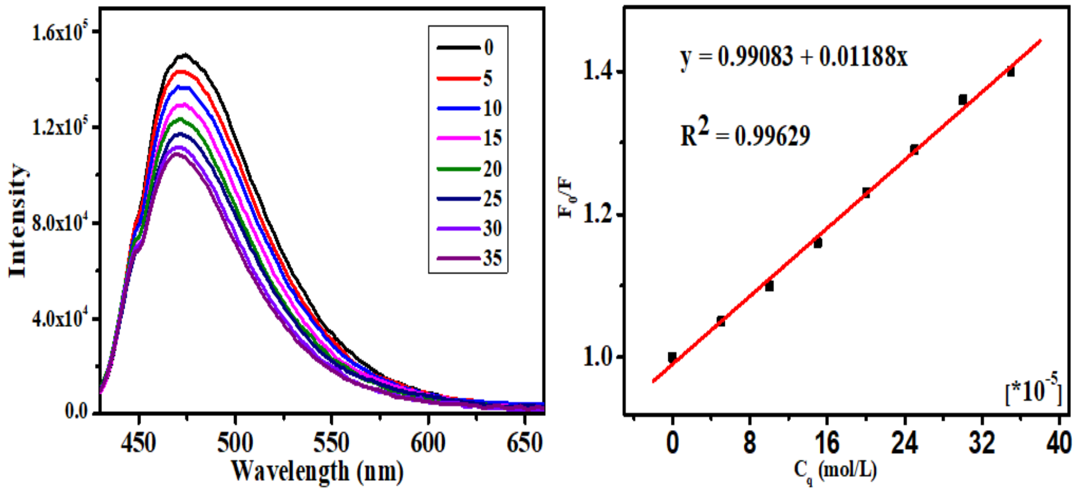

Figure S26. Fluorescence quenching spectra of Cd-**NPy**$_3$ upon the addition of 1,4-dicyanobenzene and the corresponding simulated Stern-Volmer curve.

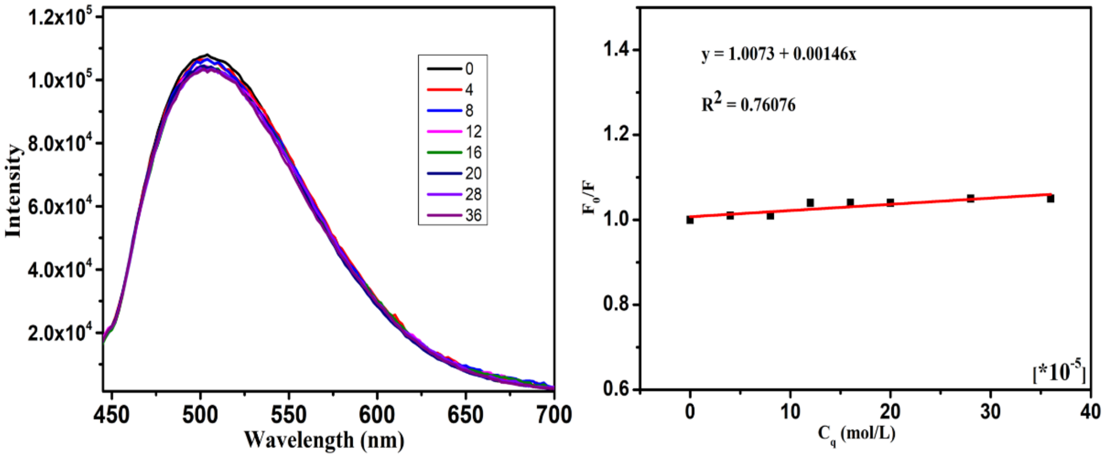

Figure S27. Fluorescence quenching spectra of Cd-**MIX** upon the addition of *N*-phenylpyrrolidine and the corresponding simulated Stern-Volmer curve.

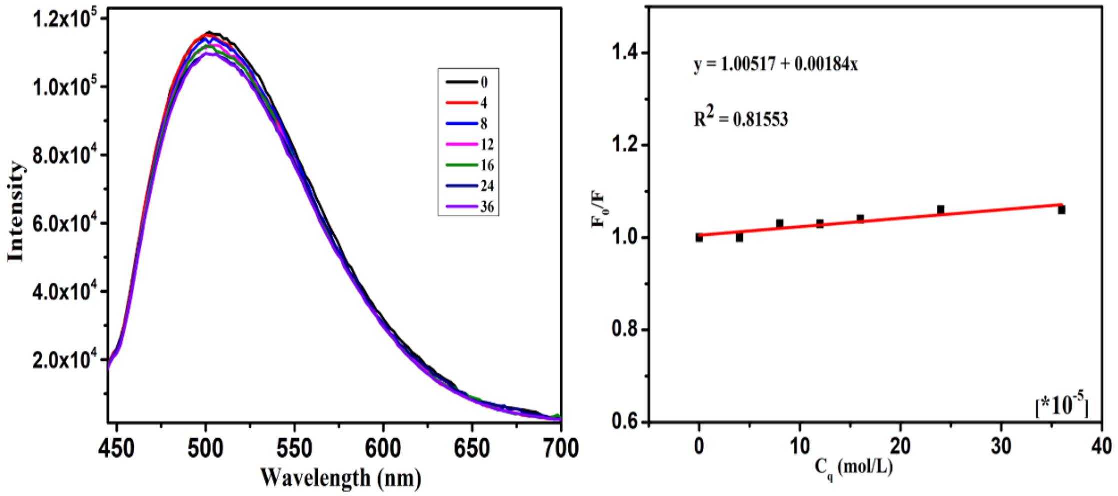

Figure S28. Fluorescence quenching spectra of Cd-**MIX** upon the addition of *N*-benzylpyrrolidine and the corresponding simulated Stern-Volmer curve.

Substrate encapsulation experiments of Cd-MIX

Firstly, Cd-**MIX** was soaked in methanol solution (48 h) for guest molecules exchange and fully dried out the methanol molecules in a vacuum oven (373 K) for 10 h. Then the impregnated crystals were obtained by soaking the Cd-**MIX** (10.0 mg) in a solution of substrate in methanol for 10 h. After the soaked Cd-**MIX** was washed with fresh methanol to remove substrate adsorbed on the surfaces of the crystals. The substrate-loaded crystals were directly used for IR spectra measurements, and digested with DMSO-d$_6$/DCl for ^{1}H NMR. The amounts of released substrate molecules were quantified by ^{1}H NMR.

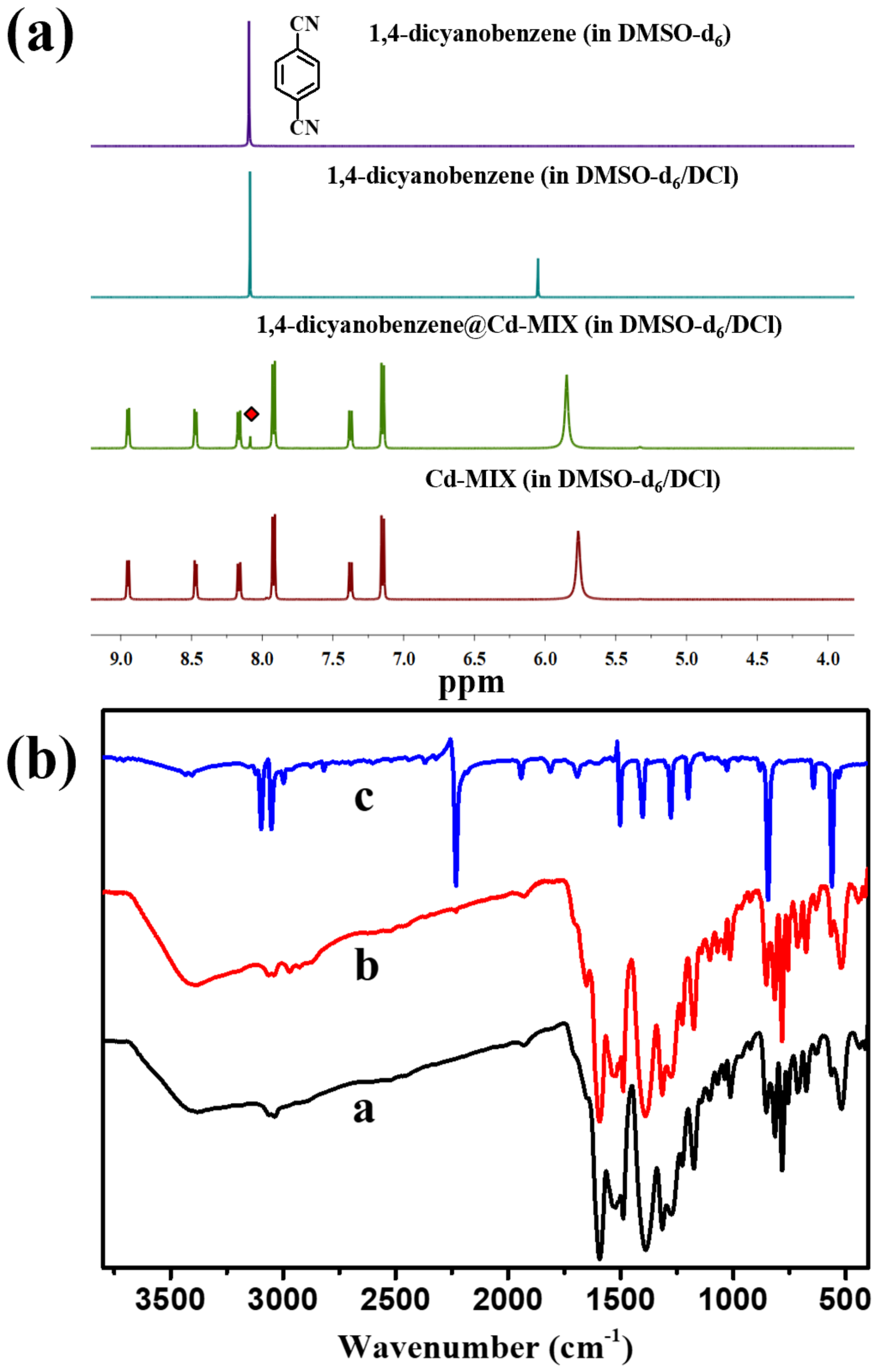

Figure S29. (a) ^{1}H NMR of Cd-**MIX**, Cd-**MIX** impregnated with 1,4-DCB, and 1,4-DCB in DMSO-d$_6$/DCl. (b) IR spectra of Cd-**MIX** (black), Cd-**MIX** impregnated with 1,4-DCB (red), and 1,4-DCB (blue).

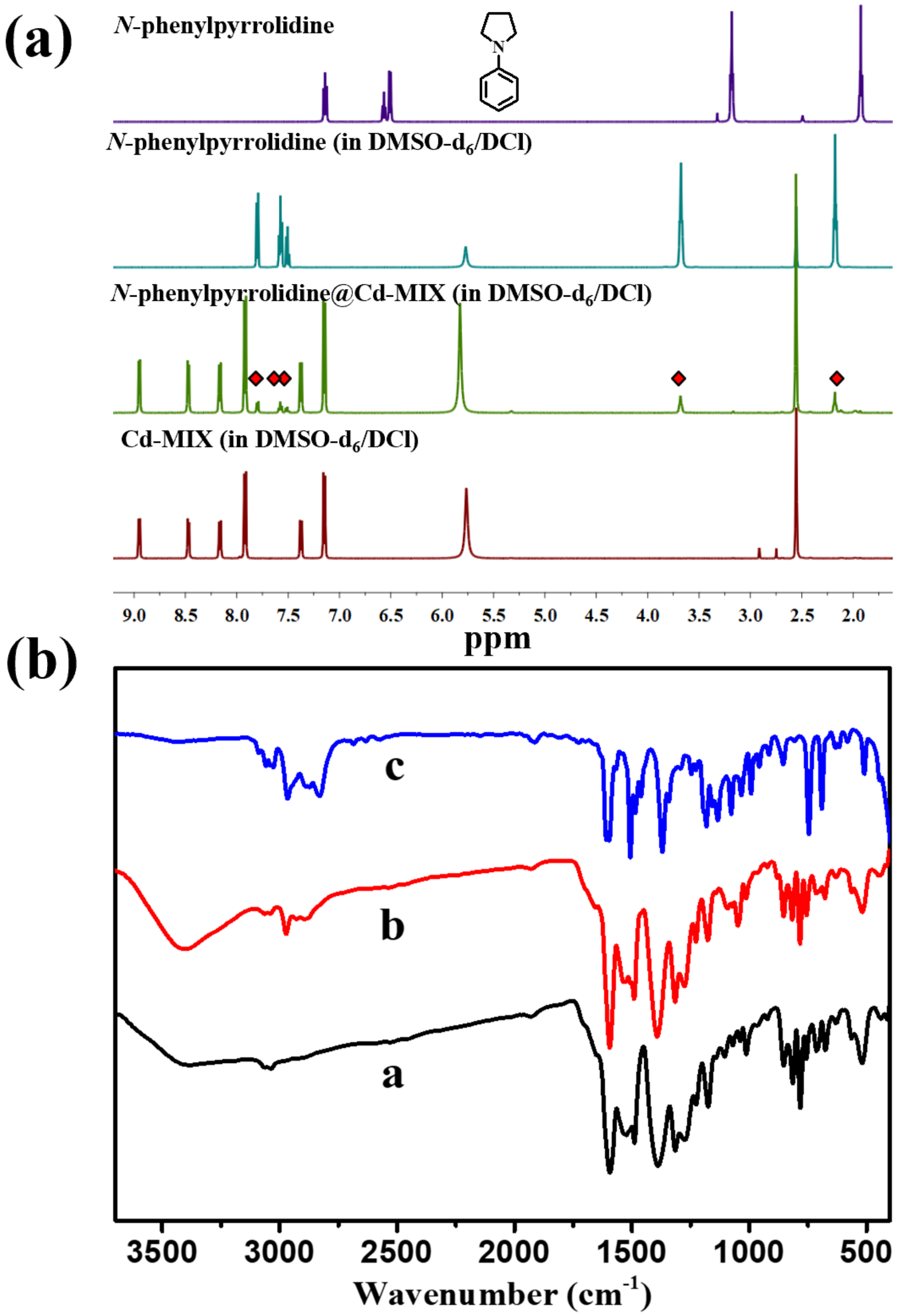

Figure S30. (a) ^{1}H NMR of Cd-**MIX**, Cd-**MIX** impregnated with *N*-phenylpyrrolidine, and *N*-phenylpyrrolidine in DMSO-d_6/DCl. (b) IR spectra of Cd-**MIX** (black), Cd-**MIX** impregnated with *N*-phenylpyrrolidine (red), and *N*-phenylpyrrolidine (blue).

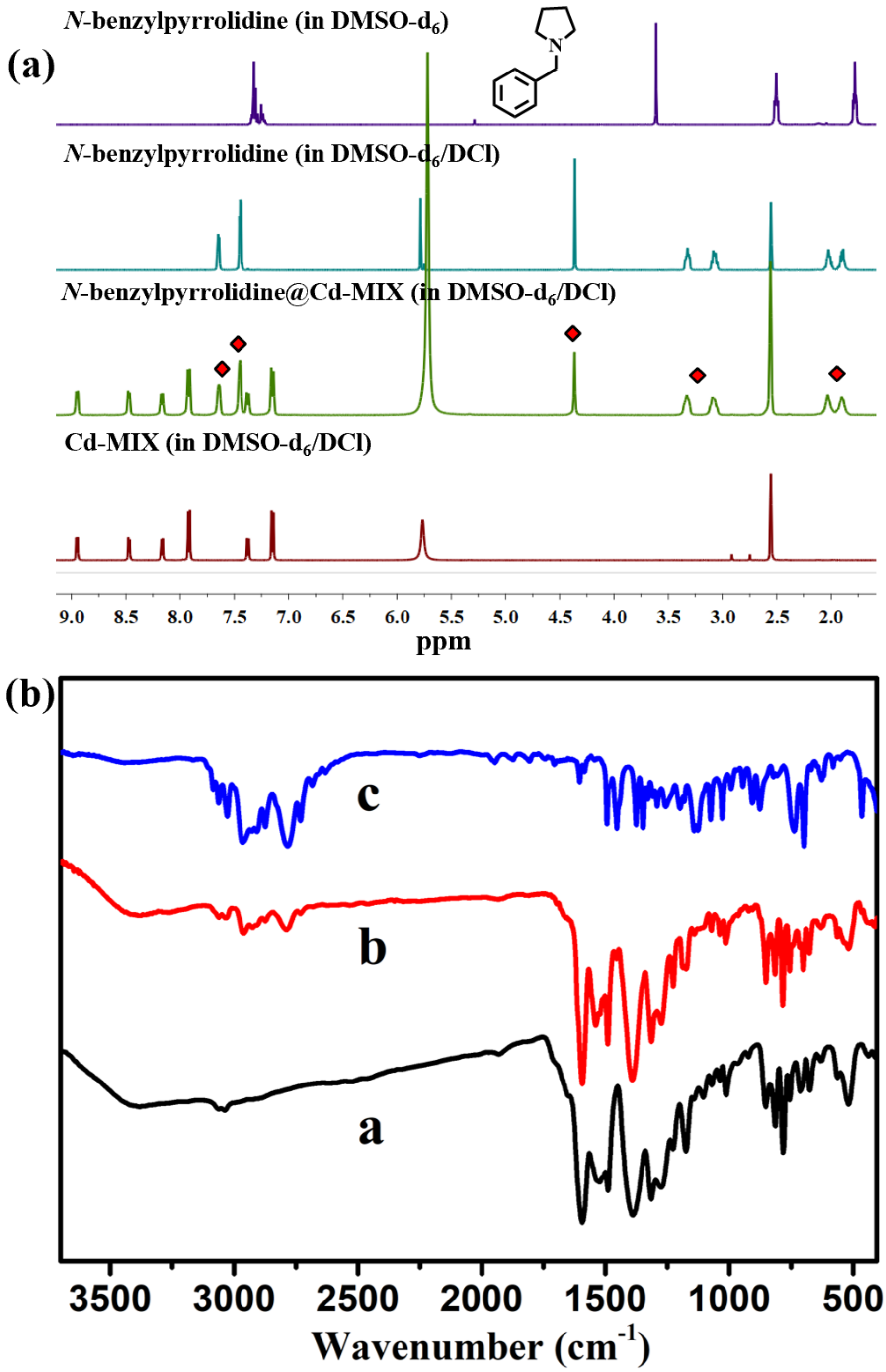

Figure S31. (a) ^{1}H NMR of Cd-**MIX**, Cd-**MIX** impregnated with *N*-benzylpyrrolidine, and *N*-benzylpyrrolidine in DMSO-d$_6$/DCl. (b) IR spectra of Cd-**MIX** (black), Cd-**MIX** impregnated with *N*-benzylpyrrolidine (red), and *N*-benzylpyrrolidine (blue).

5. Catalysis details

Table S4. The photocatalytic C–H arylation reaction under different conditions

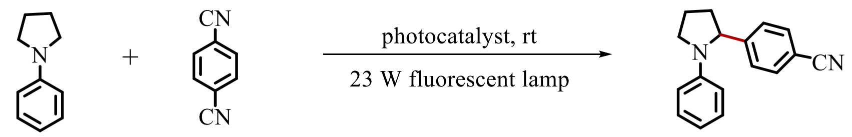

Entry	Photocatalyst	Conversion (%)[a]
1	Cd-**MIX**	96 (90[i])
2[b]	none	< 3
3	$Cd(NO_3)_2$	12
4	H_3**TCA**, **NPy_3**	18
5	$Cd(NO_3)_2$, H_3**TCA**, **NPy_3**	22
6	Cd-**TCA**	20
7	Cd-**NPy_3**	35
8	Cd-**TCA**, **NPy_3**	24
9	Cd-**NPy_3**, H_3**TCA**	37
10	Cd-**TCA**, Cd-**NPy_3**	41
11[b]	triphenylamine	< 3
12[c]	Cd-**MIX**	88
13[d]	Cd-**MIX**	46
14[e]	Cd-**MIX**	--
15[f]	Cd-**MIX / **Cd-**TCA / **Cd-**NPy_3**	>99 / >99 / >99
16[g]	Cd-**MIX / **Cd-**TCA / **Cd-**NPy_3**	96 / 41 / 50
17[h]	Cd-**MIX / **Cd-**TCA / **Cd-**NPy_3**	95 / 26 / 38

[a] Standard conditions: Cd-**MIX** (0.5 mol%, based on Ar_3N moiety, the other catalysts are based on the mole ratio of the metal and ligands in Cd-**MIX**), 1,4-dicyanobenzene (1.0 mmol), NaOAc (1.0 mmol), amine (2.0 mmol) and 4.0 mL DMAC for 12 h under N_2 atmosphere. Conversions were determined by GC-MS. [b] Take the average of three times experiments. [c] K_2HPO_4 instead of NaOAc. [d] No base. [e] Dark. [f] 365 nm LED instead of 23 W fluorescent lamp. [g] 395 nm LED instead of 23 W fluorescent lamp. [h] 420 nm LED instead of 23 W fluorescent lamp. [i] Isolated yield.

Table S5. The photocatalytic C–H arylation reaction under different conditions

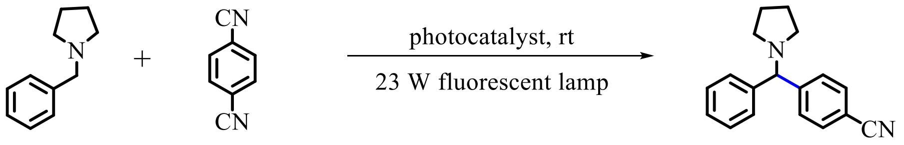

Entry	Photocatalyst	Conversion (%)[a]
1	Cd-**MIX**	98 (93[h])
2	none	--
3	$Cd(NO_3)_2$	--
4	H_3**TCA**, **NPy$_3$**	27
5	$Cd(NO_3)_2$, H_3**TCA**, **NPy$_3$**	32
6	Cd-**TCA**	16
7	Cd-**NPy$_3$**	49
8	Cd-**TCA**, **NPy$_3$**	19
9	Cd-**NPy$_3$**, H_3**TCA**	48
10	Cd-**TCA**, Cd-**NPy$_3$**	53
11	triphenylamine	--
12[b]	Cd-**MIX**	92
13[c]	Cd-**MIX**	51
14[d]	Cd-**MIX**	--
15[e]	Cd-**MIX** / Cd-**TCA** / Cd-**NPy$_3$**	>99 / >99 / >99
16[f]	Cd-**MIX** / Cd-**TCA** / Cd-**NPy$_3$**	99 / 38 / 59
17[g]	Cd-**MIX** / Cd-**TCA** / Cd-**NPy$_3$**	97 / 22 / 50

[a] Standard conditions: Cd-**MIX** (0.5 mol%, based on Ar_3N moiety, the other catalysts are based on the mole ratio of the metal and ligands in Cd-**MIX**), 1,4-dicyanobenzene (1.0 mmol), NaOAc (1.0 mmol), amine (2.0 mmol) and 4.0 mL DMSO for 10 h under N_2 atmosphere. Conversions were determined by GC-MS. [b] K_2HPO_4 instead of NaOAc. [c] No base. [d] Dark. [e] 365 nm LED instead of 23 W fluorescent lamp. [f] 395 nm LED instead of 23 W fluorescent lamp. [g] 420 nm LED instead of 23 W fluorescent lamp. [h] Isolated yield.

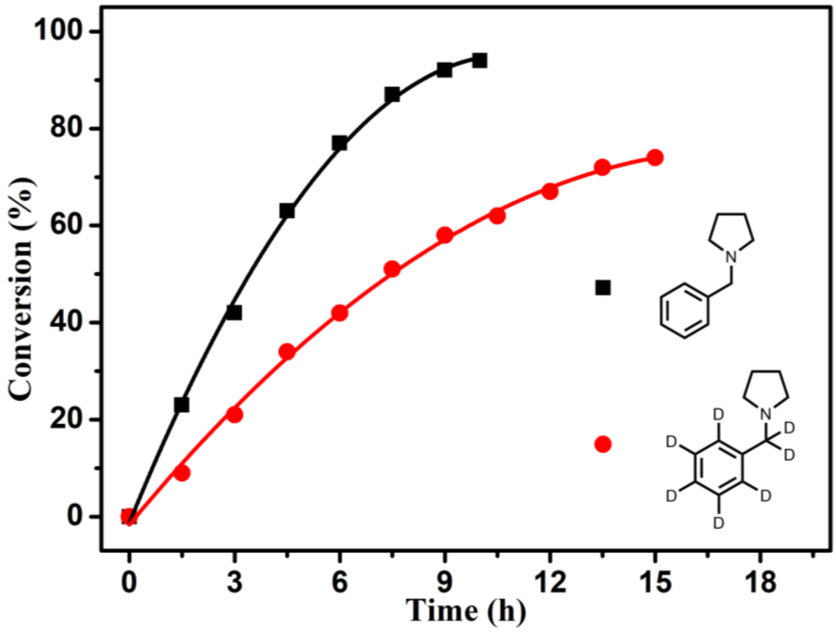

Figure S32. Kinetic curves of the C–H arylation using *N*-benzylpyrrolidine (**1c**) or *N*-((phenyl-D$_5$)methyl-D$_2$)pyrrolidine (**1c**D) with 1,4-dicyanobenzene under optimal conditions.

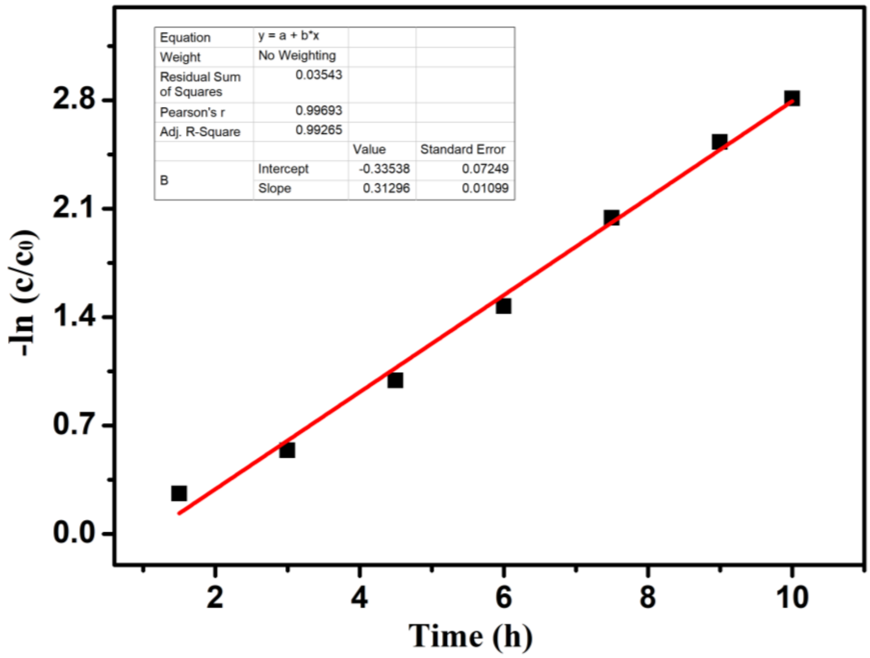

Equation	y = a + b*x		
Weight	No Weighting		
Residual Sum of Squares	0.03543		
Pearson's r	0.99693		
Adj. R-Square	0.99265		
		Value	Standard Error
B	Intercept	-0.33538	0.07249
	Slope	0.31296	0.01099

Figure S33. The fitting curve of the kinetic trace for the C(sp^3)–H functionalization reactions using *N*-benzylpyrrolidine as substrate.

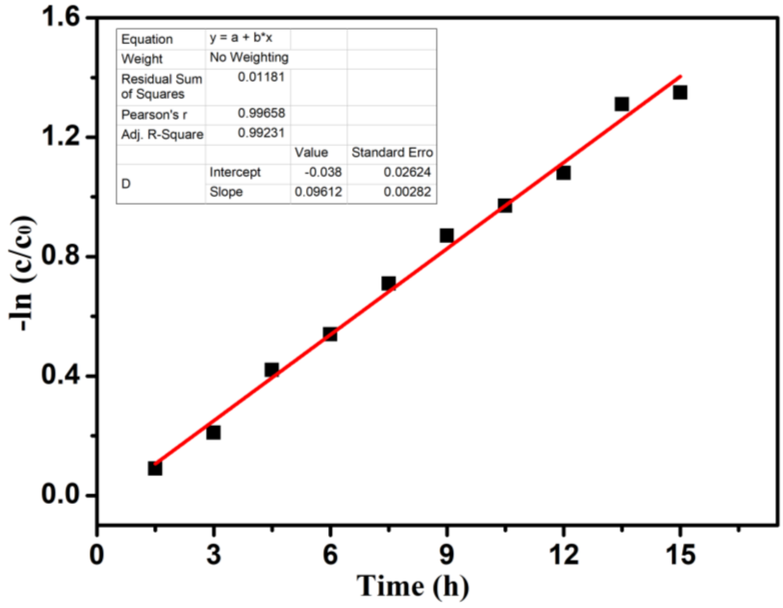

Figure S34. The fitting curve of the kinetic trace for the C(sp^3)–H functionalization reactions using *N*-((phenyl-D$_5$)methyl-D$_2$)pyrrolidine as substrate.

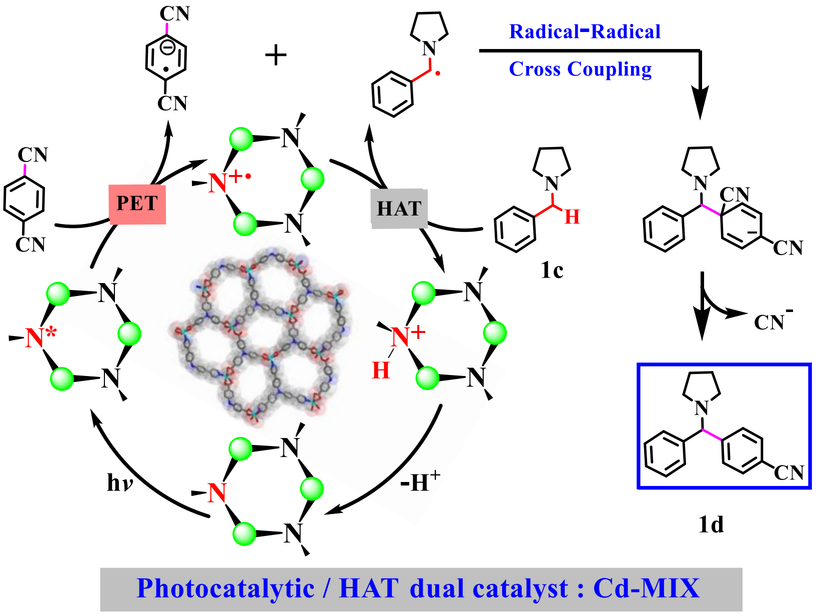

Figure S35. The proposed mechanism for regioselective C(sp^3)–H arylation reaction catalyzed by dual-functional Cd-**MIX** combining the hydrogen atom transfer and photoredox catalysis.

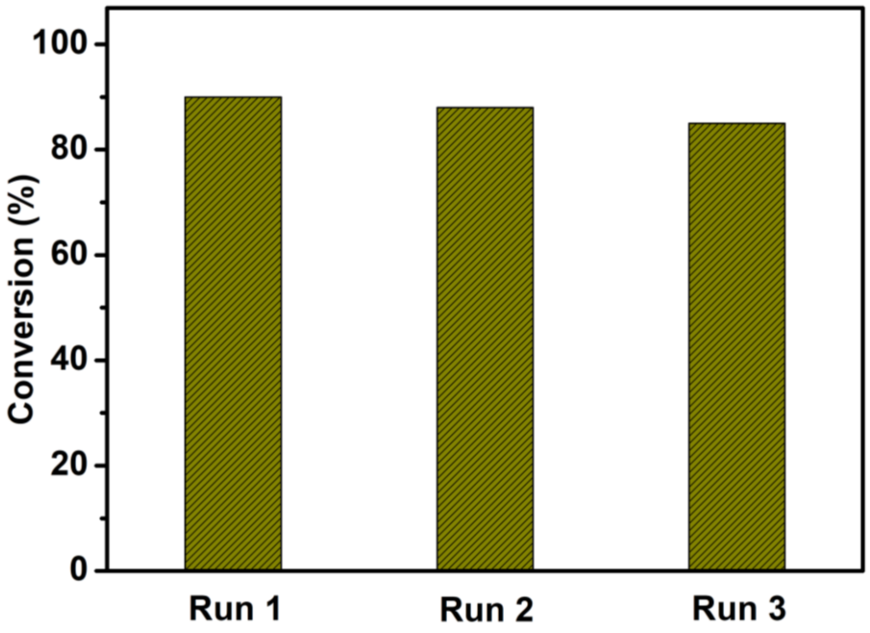

Figure S36. Recycling catalytic experiments of C–H arylation of *N*-phenylpyrrolidine (**1a**) with Cd-**MIX** as photocatalyst under optimal conditions.

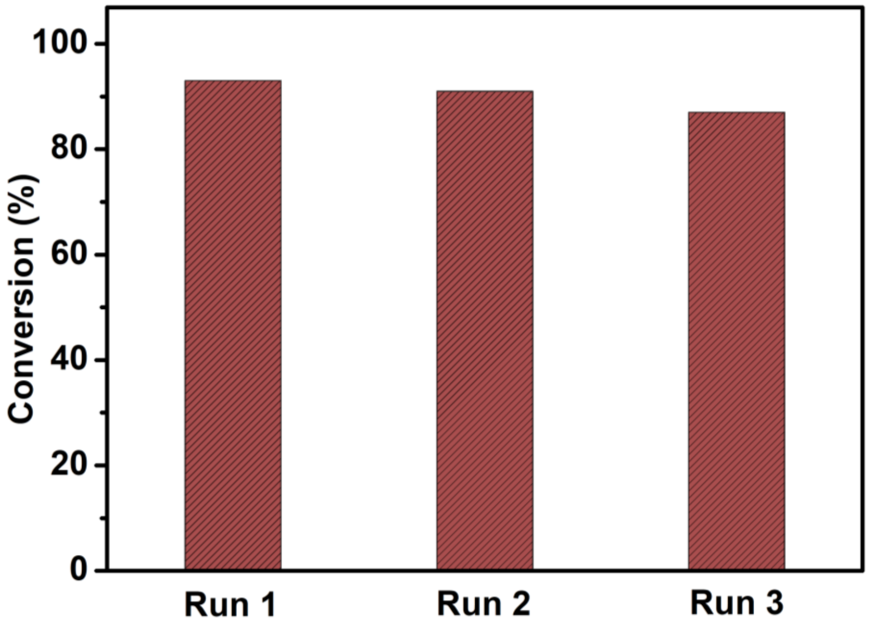

Figure S37. Recycling catalytic experiments of C–H arylation of *N*-benzylpyrrolidine (**1c**) with Cd-**MIX** as photocatalyst under optimal conditions.

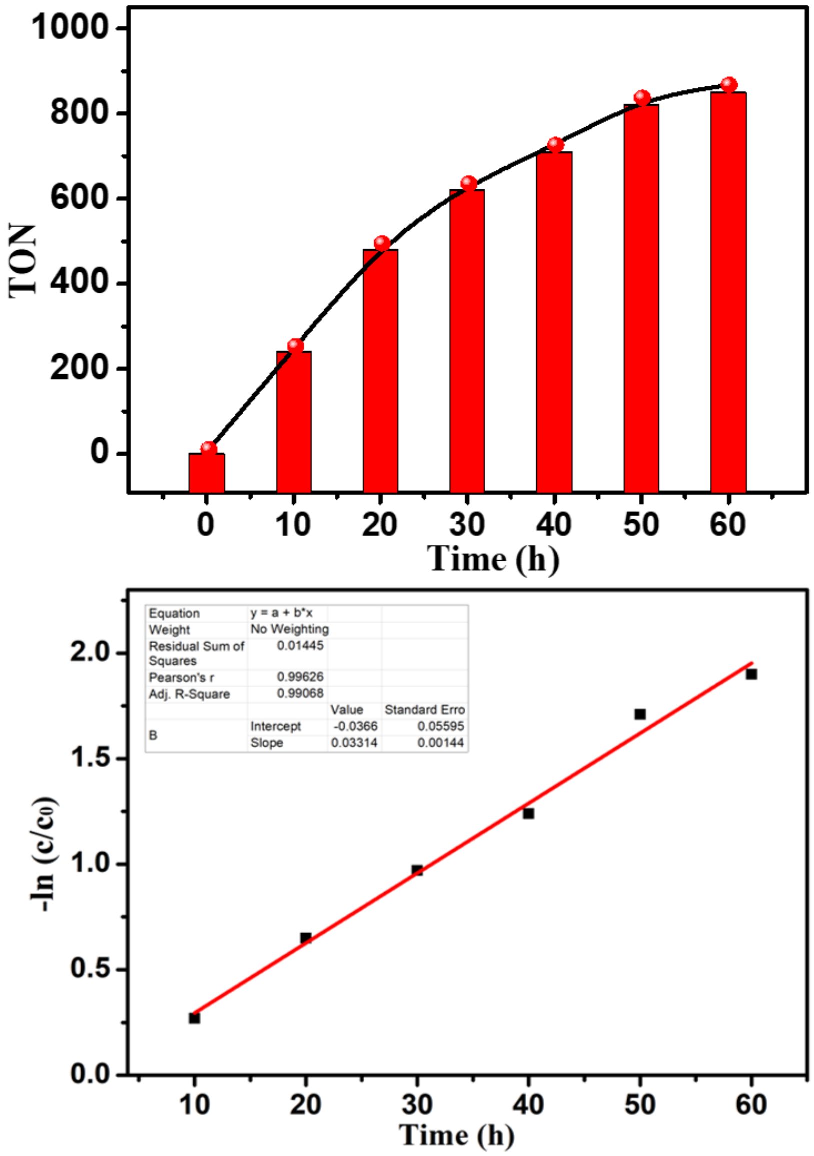

Figure S38. The turnover number during the time-course in scale-up experiments for the photocatalytic C–H arylation of *N*-phenylpyrrolidine and the corresponding fitting curve. Reaction condition: 1,4-dicyanobenzene (5.0 mmol, 1.0 equiv), photocatalyst (0.1 mol%, based on Ar$_3$N moiety in Cd-**MIX**), NaOAc (5.0 mmol, 1.0 equiv), amine (10.0 mmol, 2.0 equiv) and DMAC (20.0 mL). Then the reaction mixture was cooled to –78 ℃, degassed and backfilled with N$_2$ for three times. The resulting mixture was stirred and irradiated with 23 W fluorescent lamp at room temperature for 60 h.

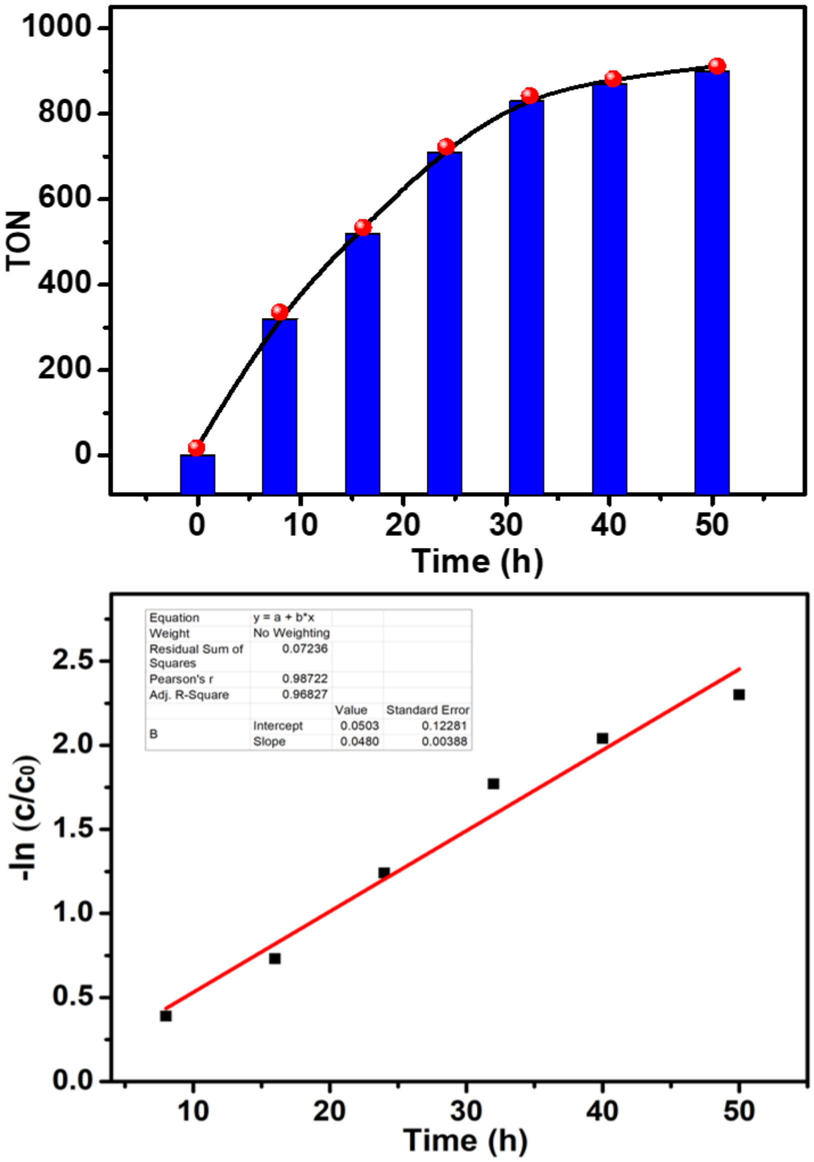

Equation	y = a + b*x		
Weight	No Weighting		
Residual Sum of Squares	0.07236		
Pearson's r	0.98722		
Adj. R-Square	0.96827		
		Value	Standard Error
B	Intercept	0.0503	0.12281
	Slope	0.0480	0.00388

Figure S39. The turnover number during the time-course in scale-up experiments for the photocatalytic C–H arylation of *N*-benzylpyrrolidine and the corresponding fitting curve. Reaction condition: 1,4-dicyanobenzene (5.0 mmol, 1.0 equiv), photocatalyst (0.1 mol%, based on Ar_3N moiety in Cd-**MIX**), NaOAc (5.0 mmol, 1.0 equiv), amine (10.0 mmol, 2.0 equiv) and DMSO (20.0 mL). Then the reaction mixture was cooled to –78 ℃, degassed and backfilled with N_2 for three times. The resulting mixture was stirred and irradiated with 23 W fluorescent lamp at room temperature for 50 h.

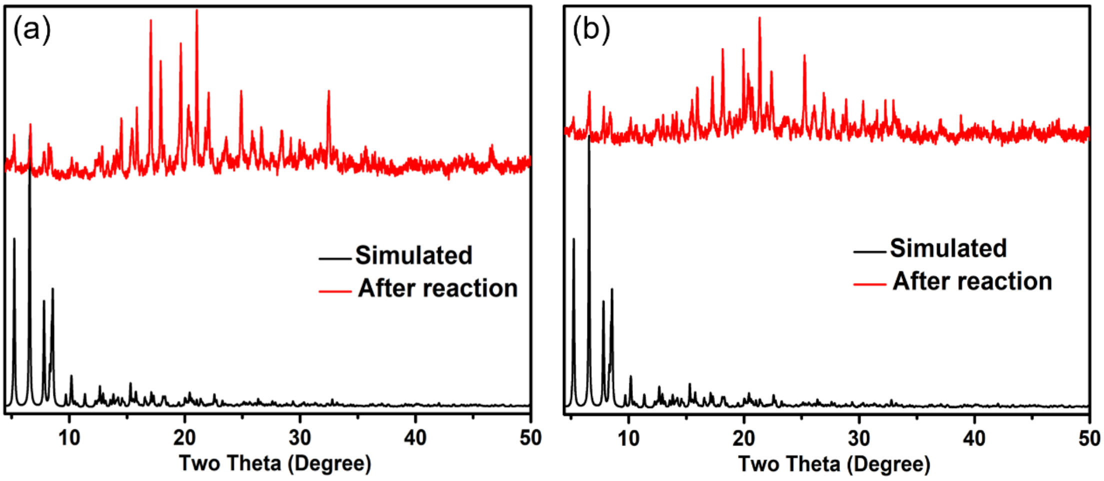

Figure S40. PXRD patterns of Cd-**MIX** showing the calculated pattern based on the single-crystal (black) and the post-catalysis Cd-**MIX** after 3 runs experiments (a) and scale-up experiments (b).

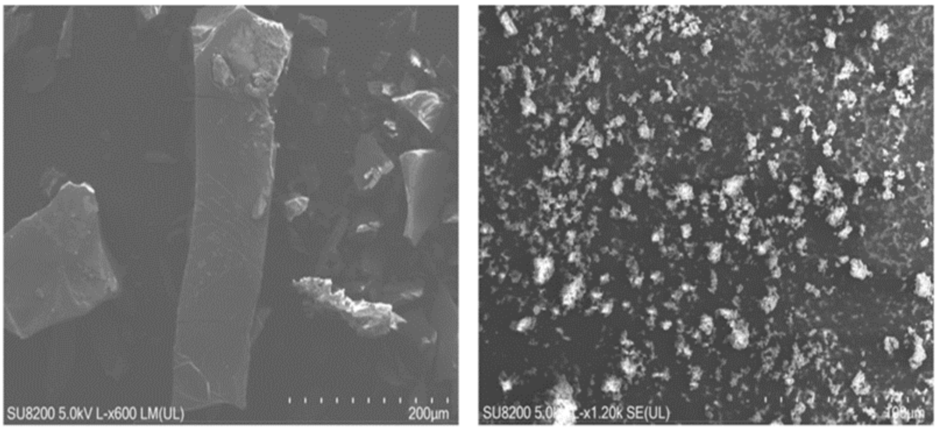

Figure S41. SEM images of the initial crystals of Cd-**MIX** with size about 200 μm (left), with the catalytic conversion of 90% using *N*-phenylpyrrolidine as substrate and 93% using *N*-benzylpyrrolidine as substrate under optimal conditions; and the fine crystalline materials with size 0.5~1.0 μm (right) by grinding of Cd-**MIX** with the catalytic conversion of 89% using *N*-phenylpyrrolidine as substrate and 90% using *N*-benzylpyrrolidine as substrate under optimal conditions.

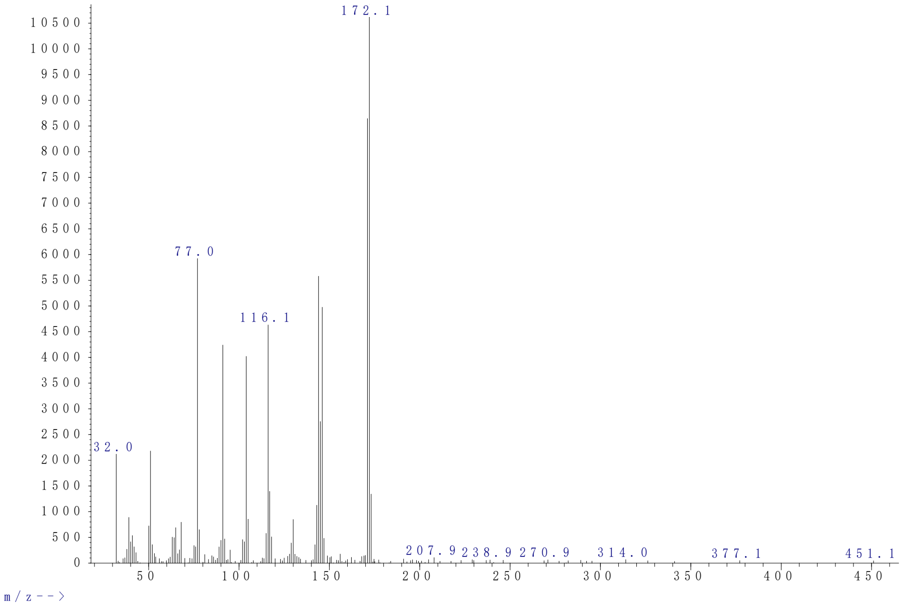

Figure S42. Mass spectrum of the possible byproducts (1-phenylpyrrolidine-2-carbonitrile) after a 365 nm LED irradiation for the C–H arylation with **1a** as coupling substrate under optimal conditions.

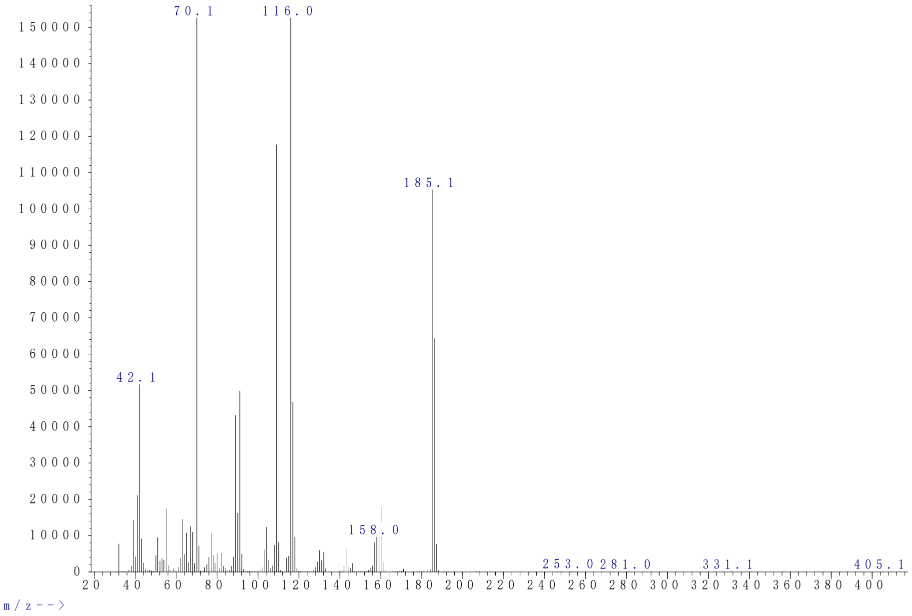

Figure S43. Mass spectrum of the possible byproducts (2-phenyl-2-(pyrrolidin-1-yl)acetonitrile) after a 365 nm LED irradiation for the C–H arylation with **1c** as coupling substrate under optimal conditions.

6. References

[S1] P. Y. Wu, C. He, J. Wang, X. J. Peng, X. Z. Li, Y. L. An and C. Y. Duan, *J. Am. Chem. Soc.*, 2012, **134**, 14991–14999.

[S2] C. Hua, A. Baldansuren, F. Tuna, D. Collison and D. M. D'Alessandro, *Inorg. Chem.*, 2016, **55**, 7270–7280.

[S3] Y. Shen, X. F. Yang, H. B. Zhu, Y. Zhao and W. S. Li, *Dalton Trans*. 2015, **44**, 14741–14746.

[S4] SMART, Data collection software (version 5.629) (Bruker AXS Inc., Madison, WI, 2003).

[S5] SAINT, Data reduction software (version 6.54) (Bruker AXS Inc., Madison, WI, 2003).

[S6] G. M. Sheldrick, SHELXTL97, Program for crystal structure solution (University of Göttingen: Göttingen, Germany, 1997).

[S7] H. Zhao, *J. Label Compd. Radiopharm.*, 2008, **51**, 293–296.

[S8] K. Muralirajan, R. Kancherla, and M. Rueping, *Angew. Chem. Int. Ed.*, 2018, **57**, 14787–14791.

Supporting Information Spectra

^{1}H NMR (400 MHz, DMSO-d$_6$/DCl) spectrum of 1,4-dicyanobenzene

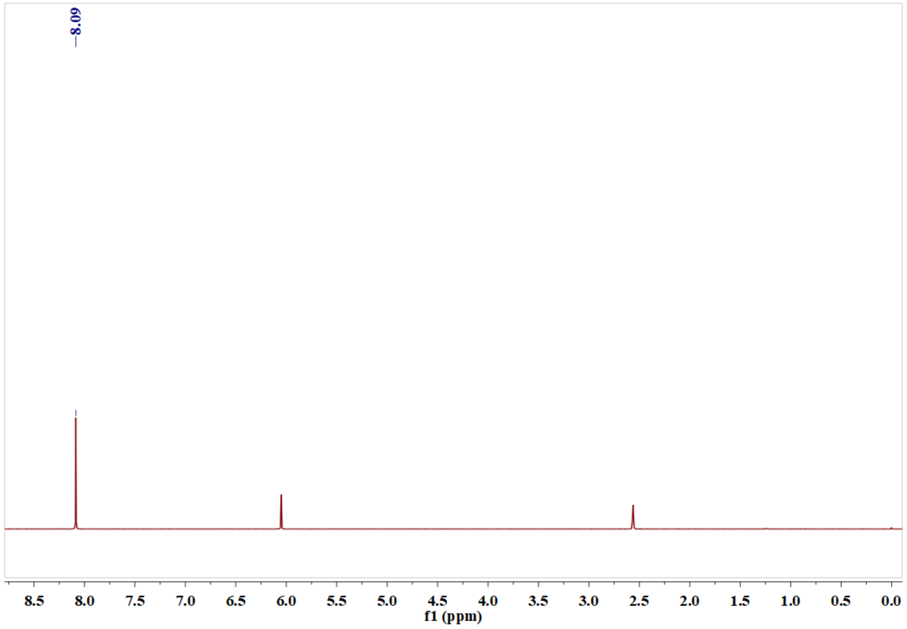

^{1}H NMR (400 MHz, DMSO-d$_6$/DCl) spectrum of *N*-phenylpyrrolidine

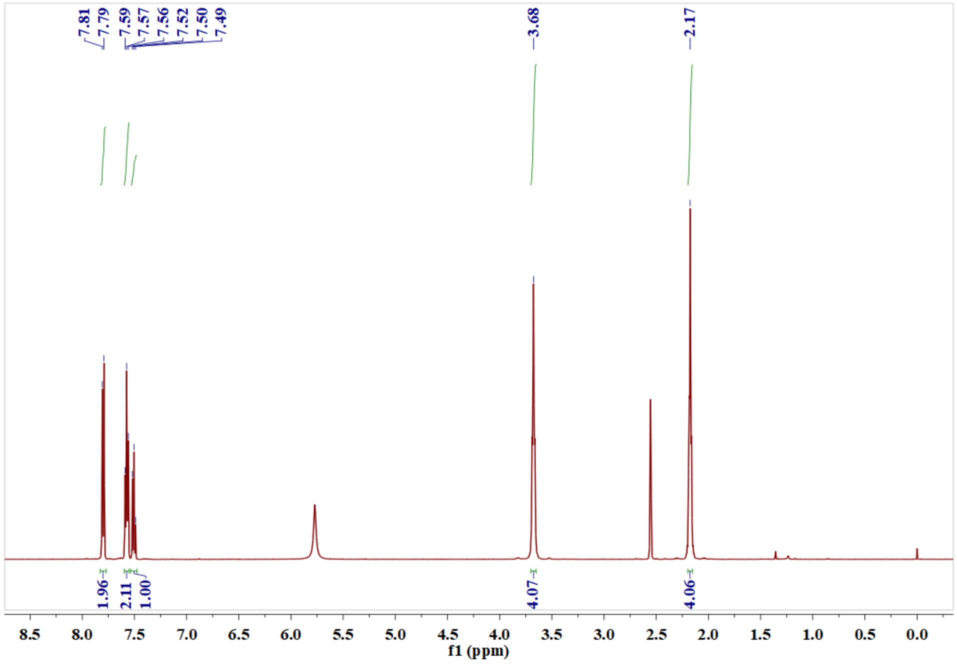

^{1}H NMR (400 MHz, DMSO-d$_6$/DCl) spectrum of *N*-benzylpyrrolidine

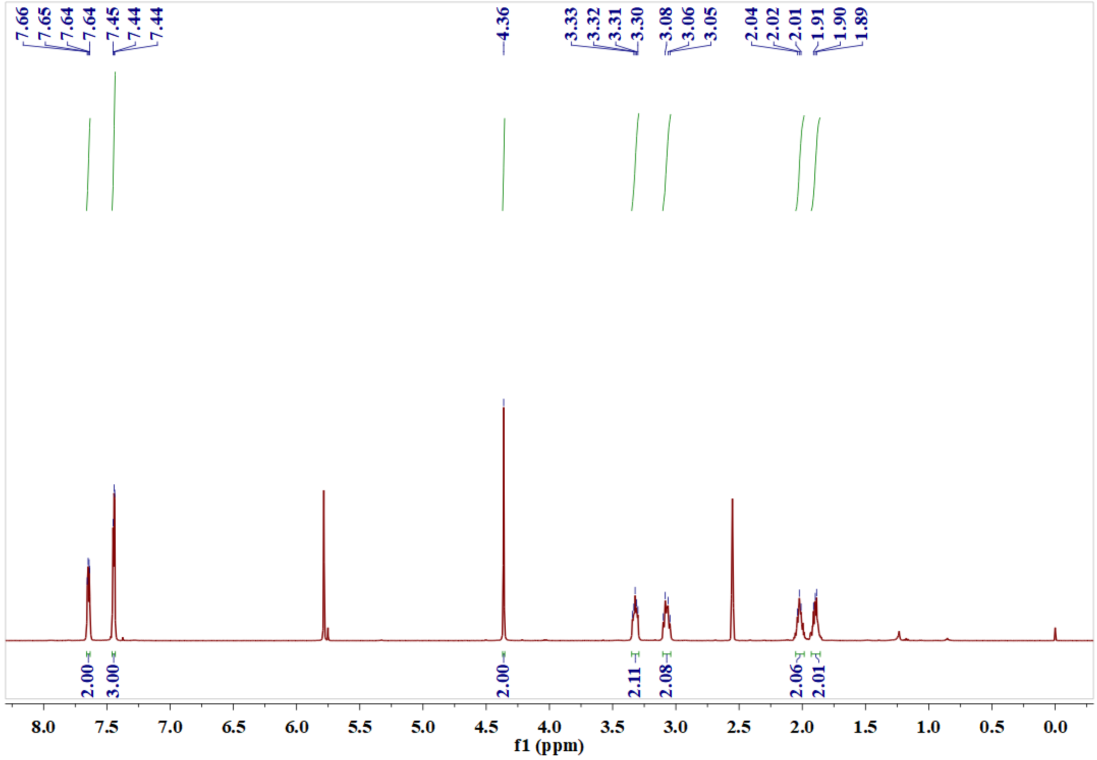

GC-MS spectrum of [D$_7$]benzyl bromide

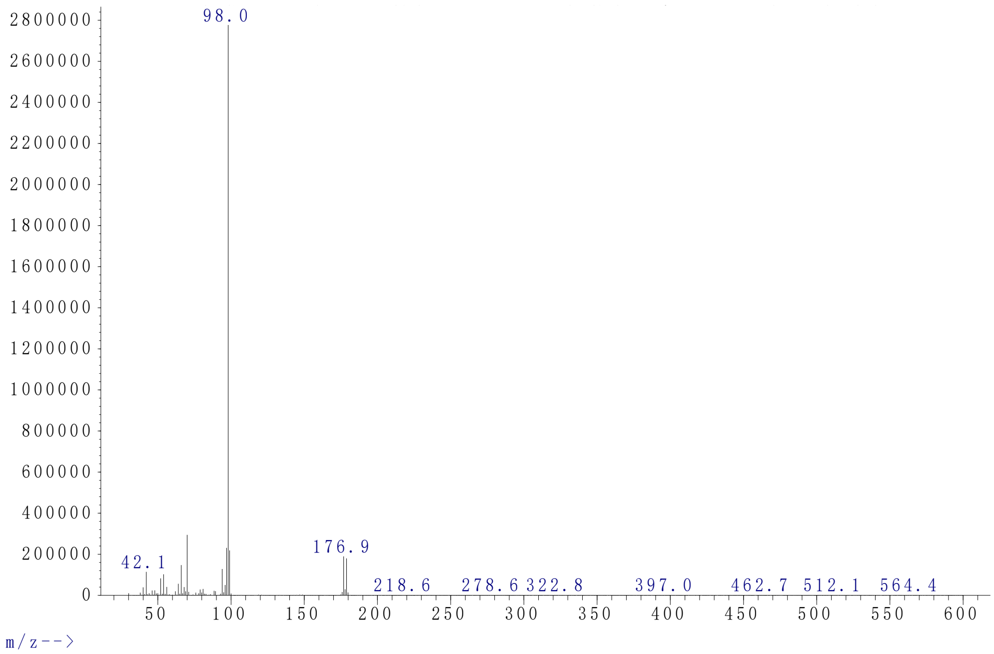

^1H NMR (400 MHz, $CDCl_3$-d_1) spectrum of 1cD

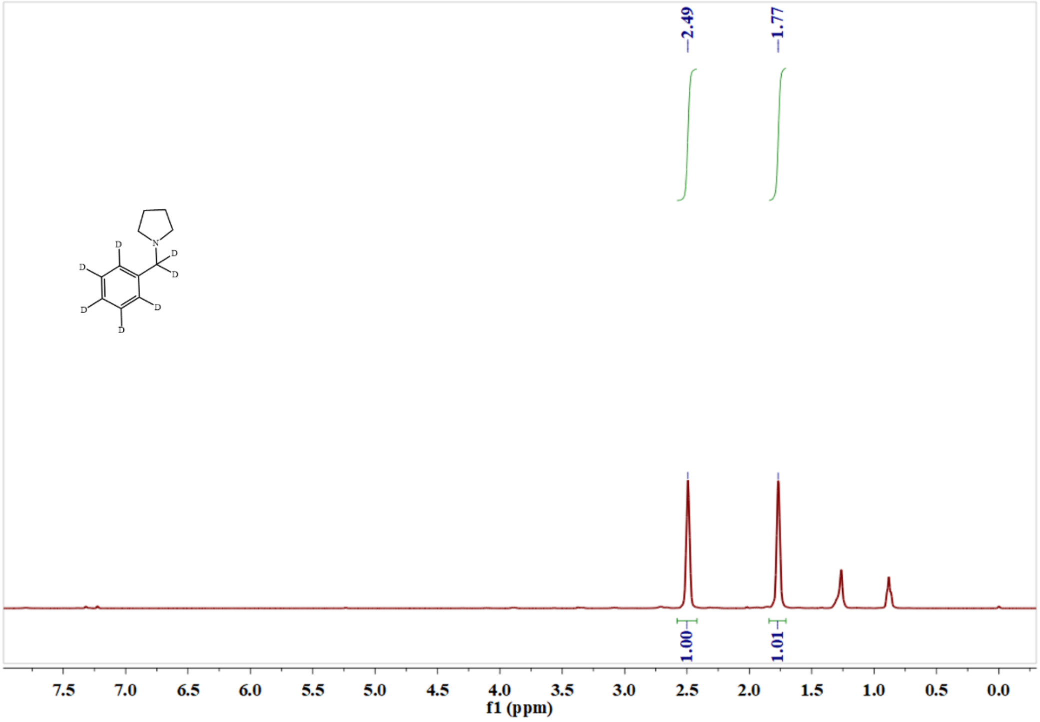

^{13}C NMR (100 MHz, $CDCl_3$-d_1) spectrum of 1cD

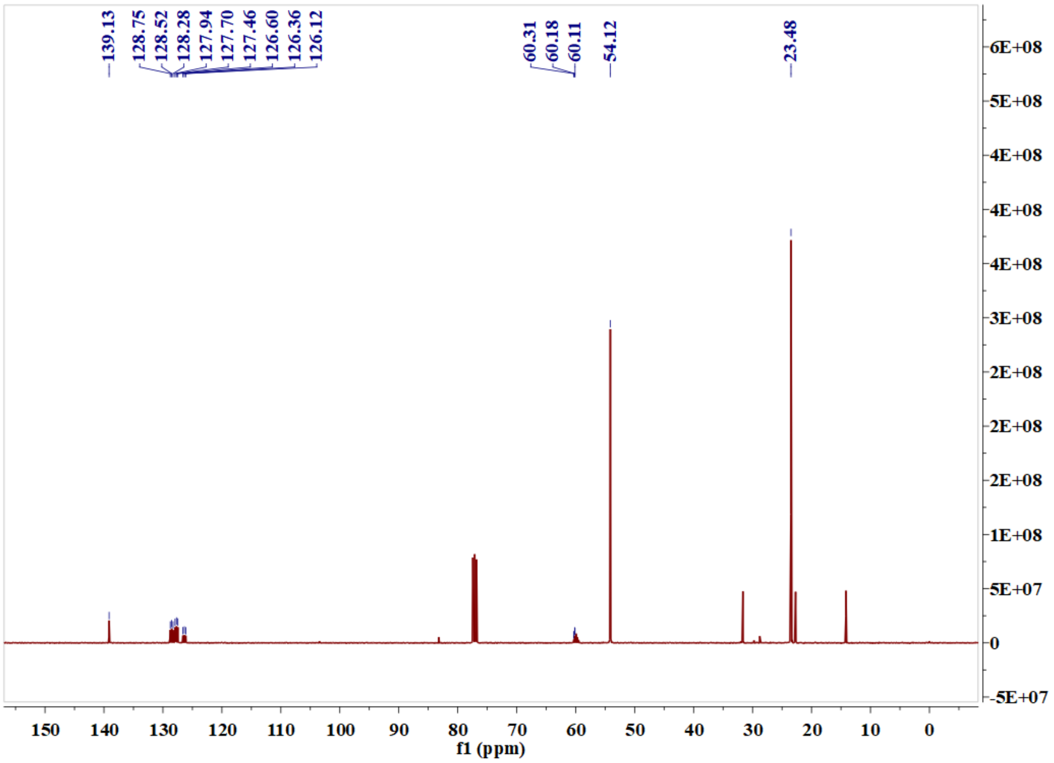

GC-MS spectrum of 1cD

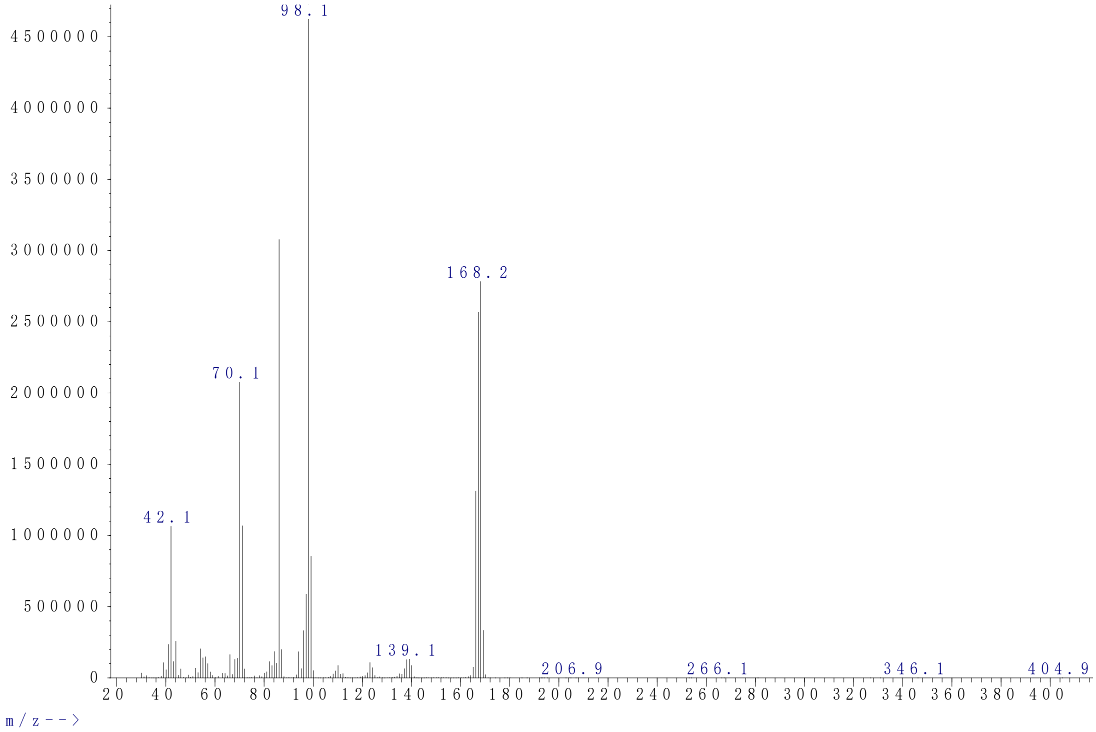

^{1}H NMR (400 MHz, $CDCl_3$-d_1) spectrum of 1dD

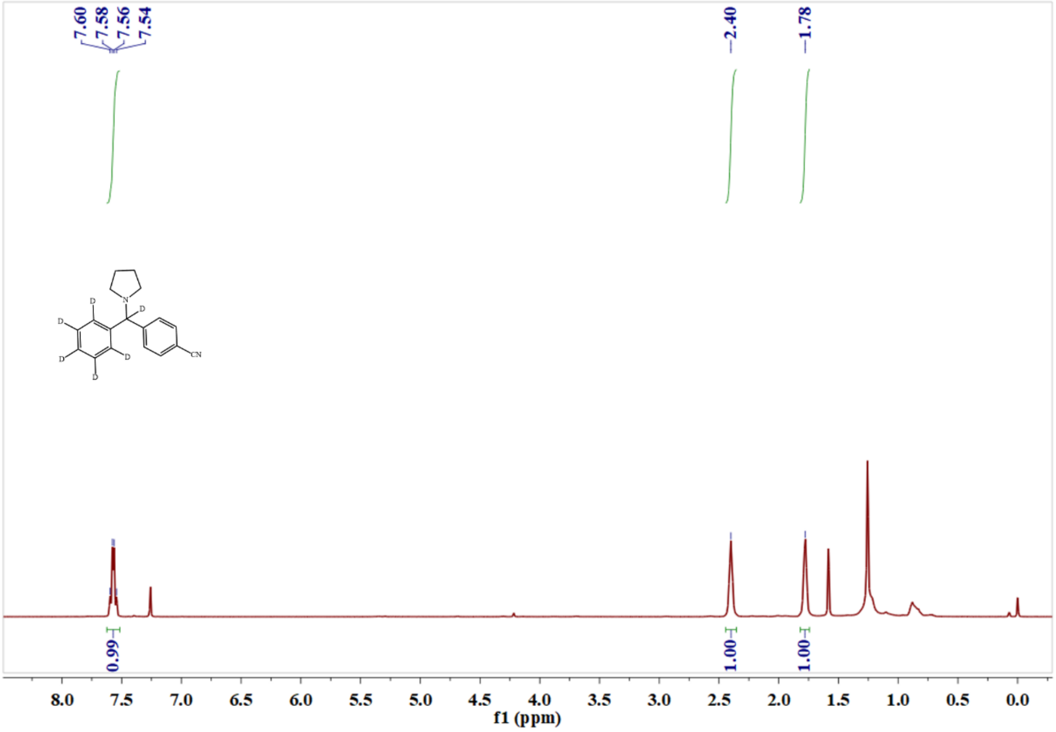

^{13}C NMR (100 MHz, $CDCl_3$-d_1) spectrum of 1dD

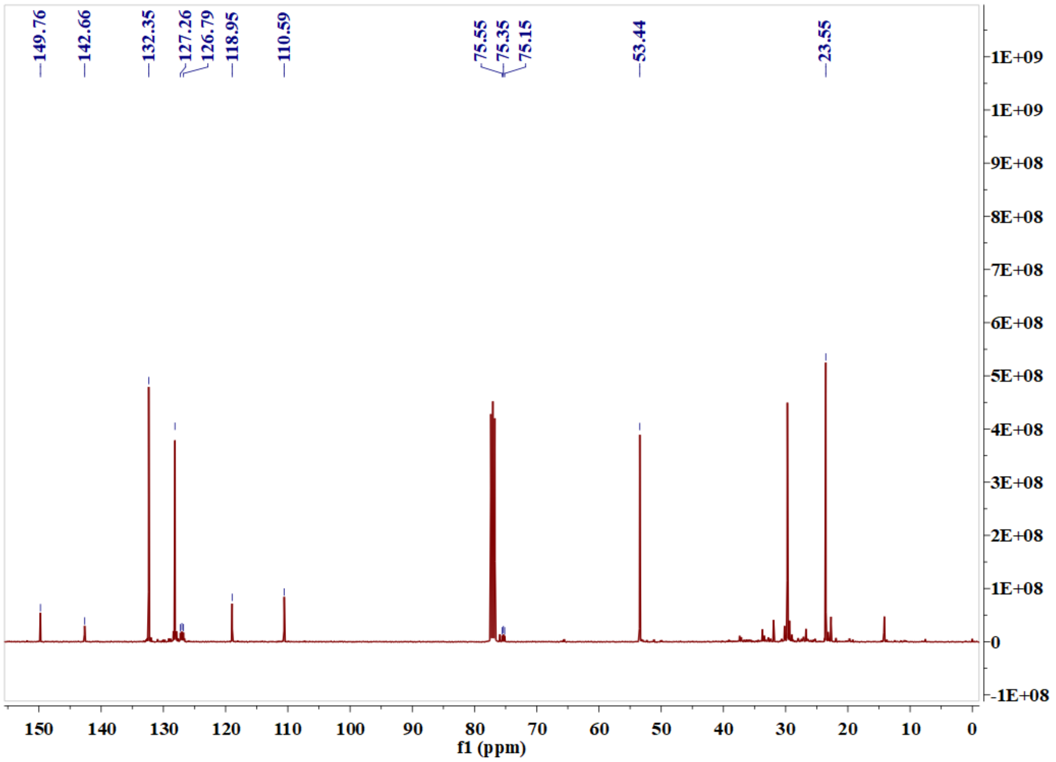

ESI-MS spectrum of 1dD

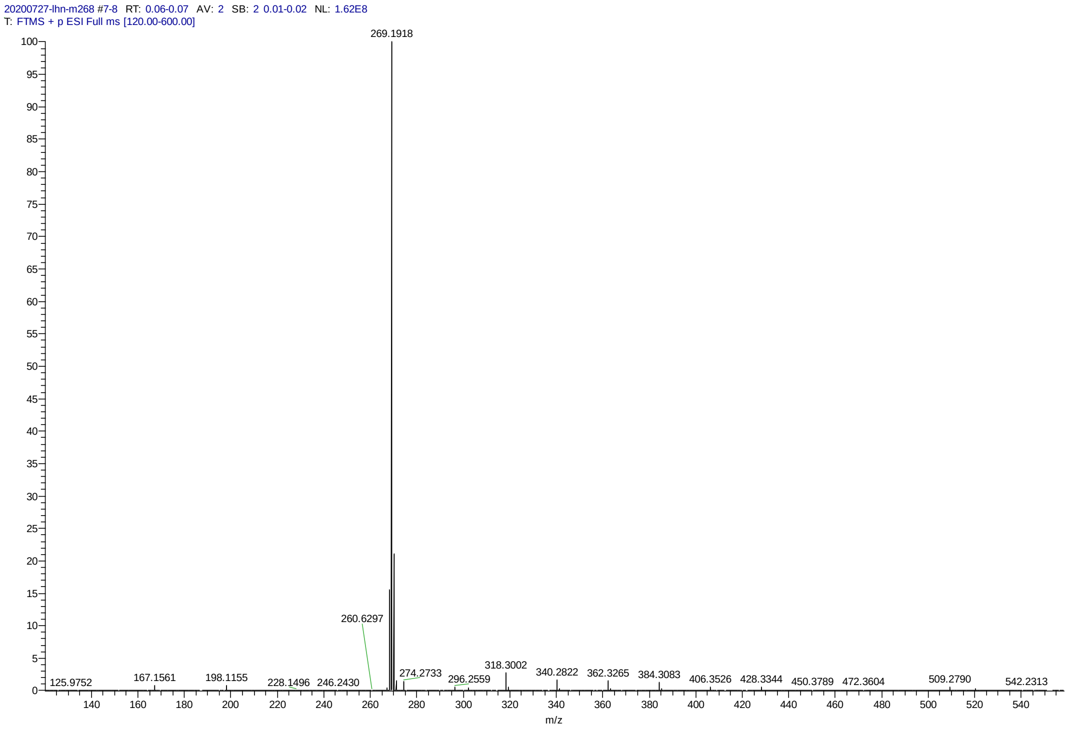

^{1}H NMR (400 MHz, CDCl$_3$-d$_1$) spectrum of 1b

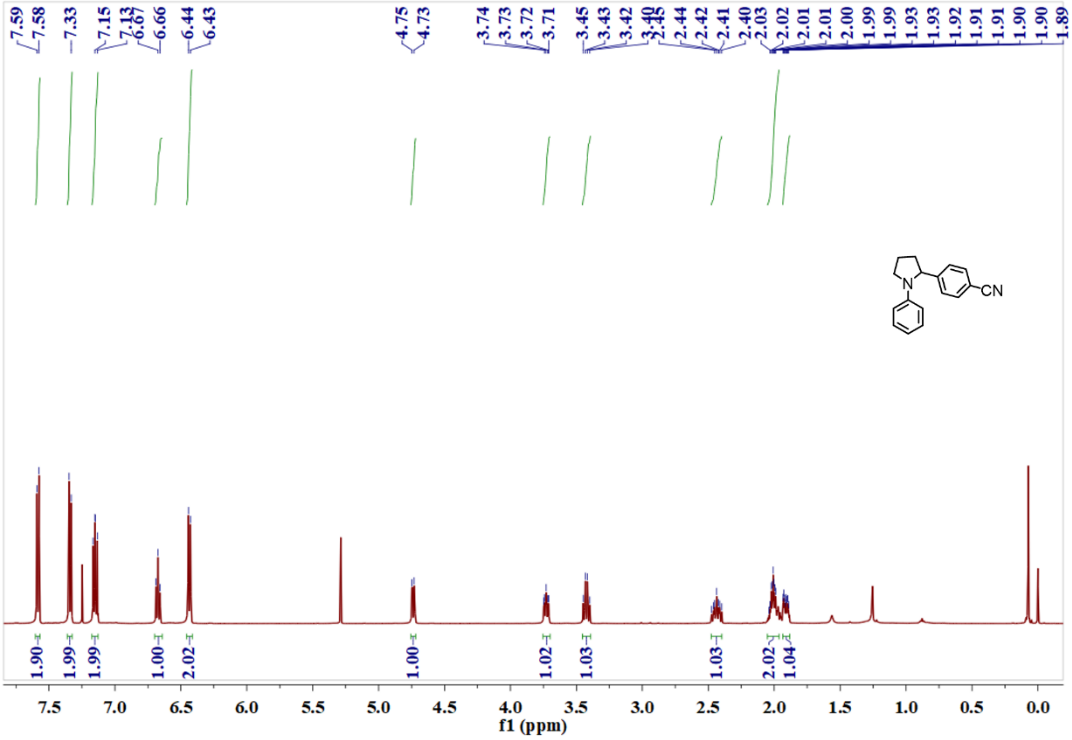

^{1}H NMR (400 MHz, CDCl$_3$-d$_1$) spectrum of 2b

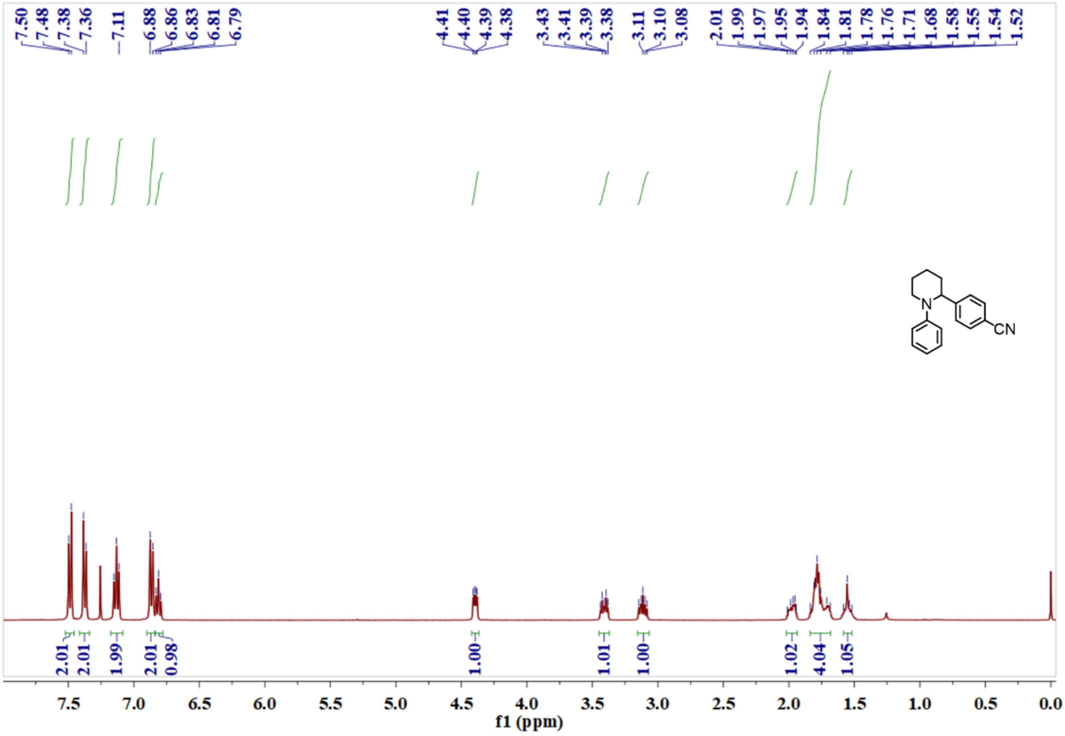

^{1}H NMR (400 MHz, $CDCl_3$-d_1) spectrum of 3b

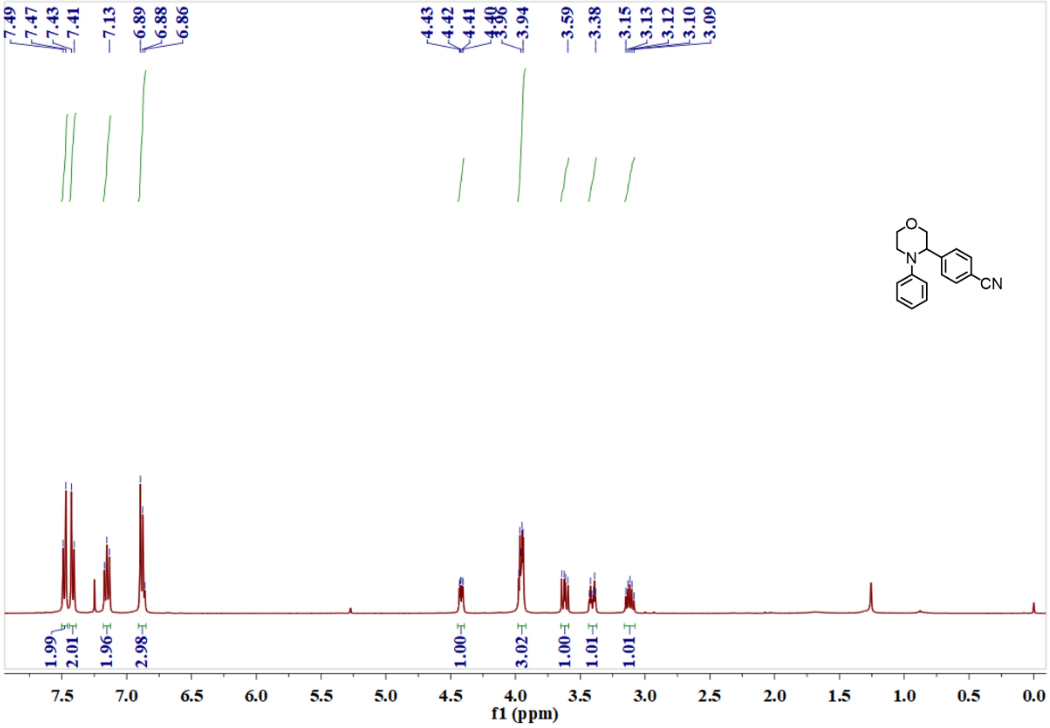

^{1}H NMR (400 MHz, $CDCl_3$-d_1) spectrum of 4b

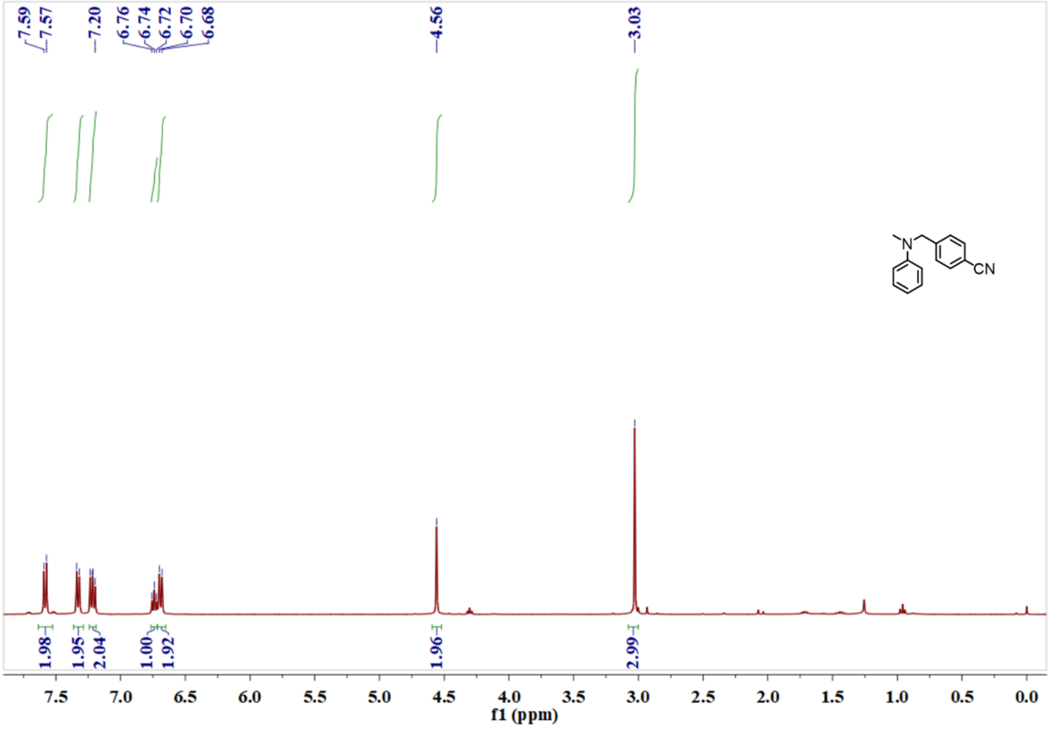

^{1}H NMR (400 MHz, CDCl$_3$-d$_1$) spectrum of 5b

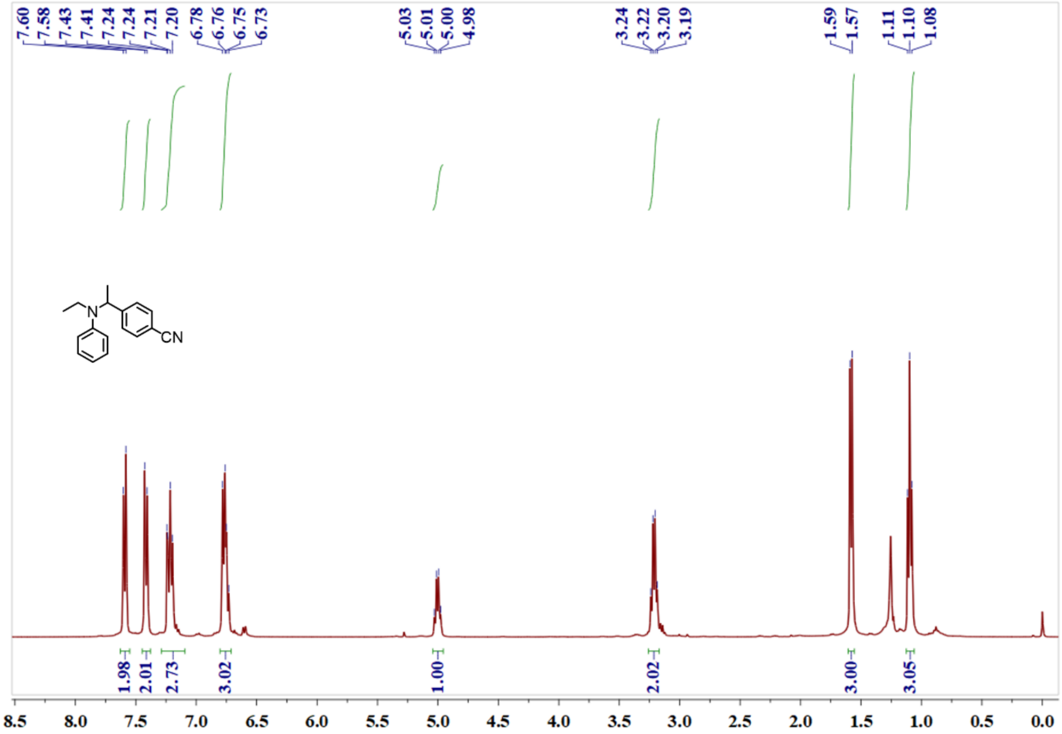

^{1}H NMR (400 MHz, CDCl$_3$-d$_1$) spectrum of 1d

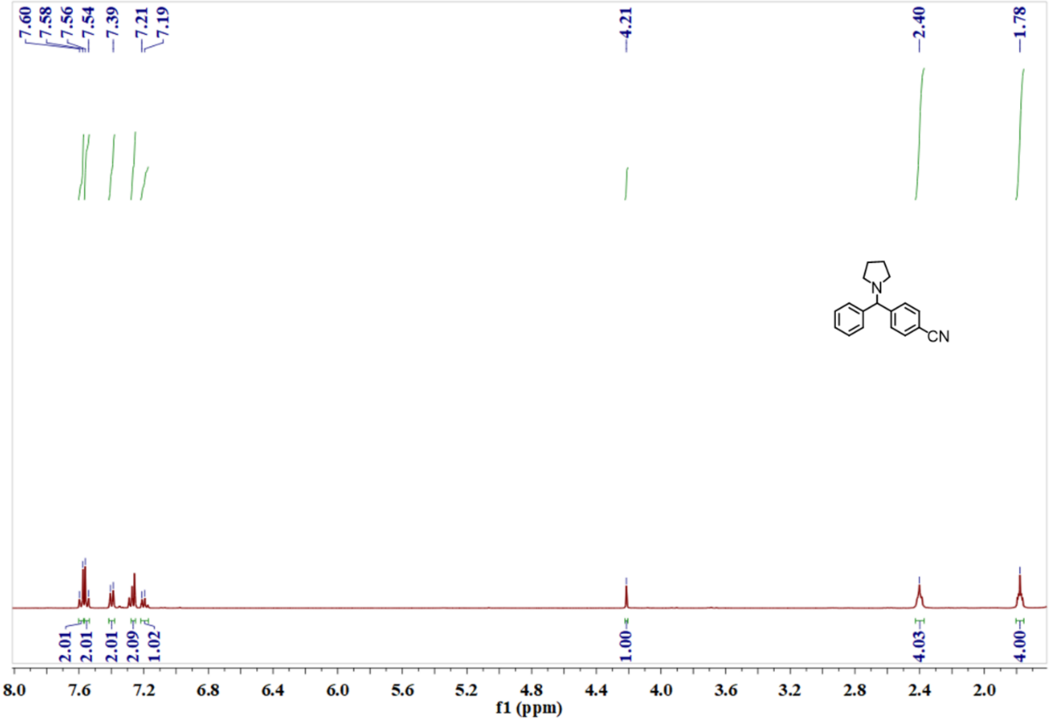

^{1}H NMR (400 MHz, CDCl$_3$-d$_1$) spectrum of 2d

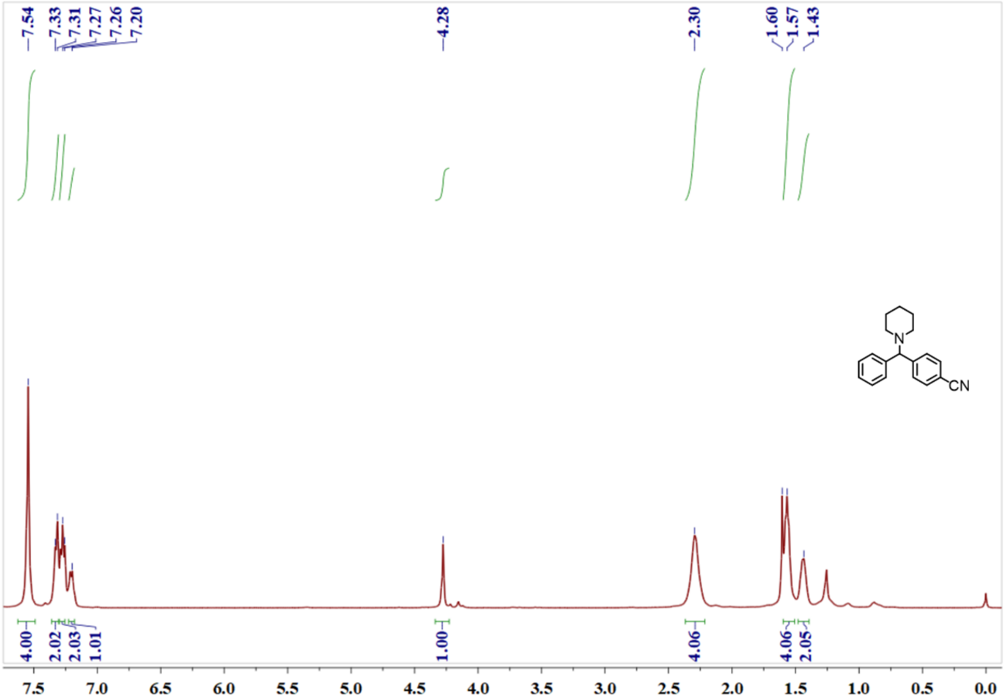

^{1}H NMR (400 MHz, CDCl$_3$-d$_1$) spectrum of 3d

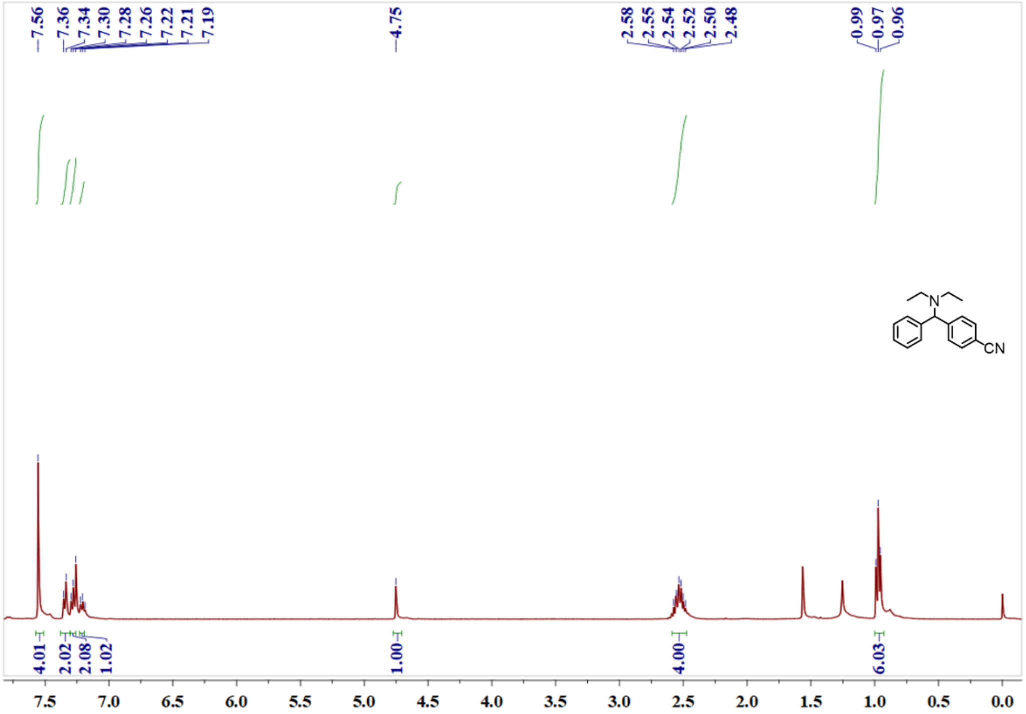

^{1}H NMR (400 MHz, CDCl$_3$-d$_1$) spectrum of 4d

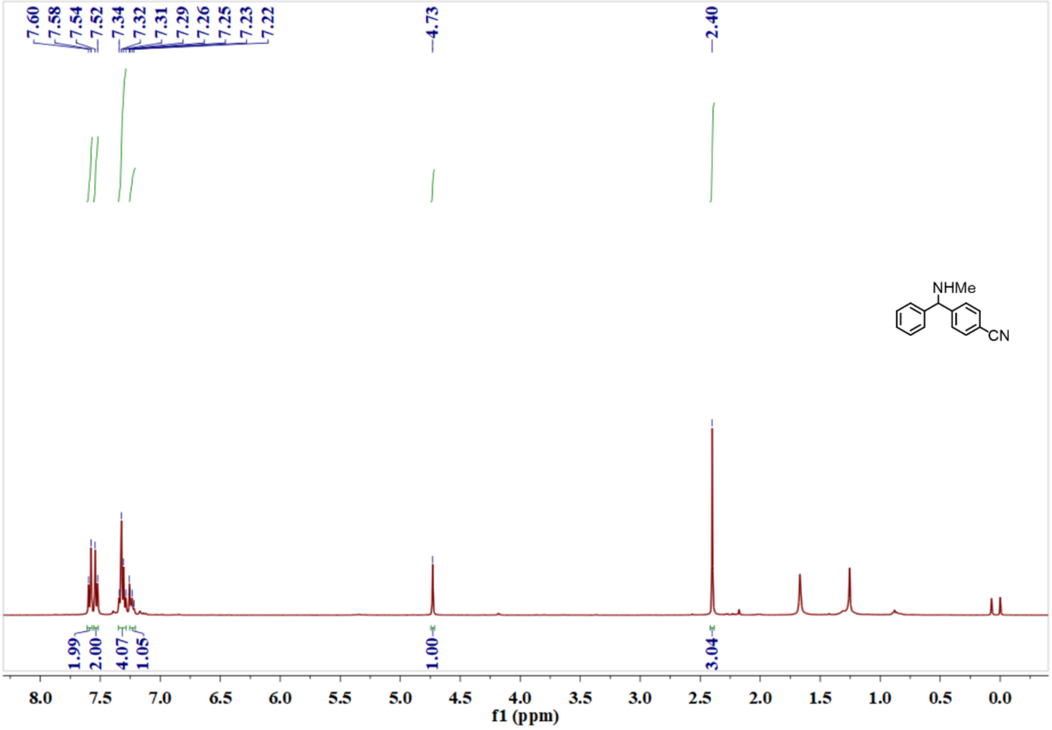

^{1}H NMR (400 MHz, CDCl$_3$-d$_1$) spectrum of 5d

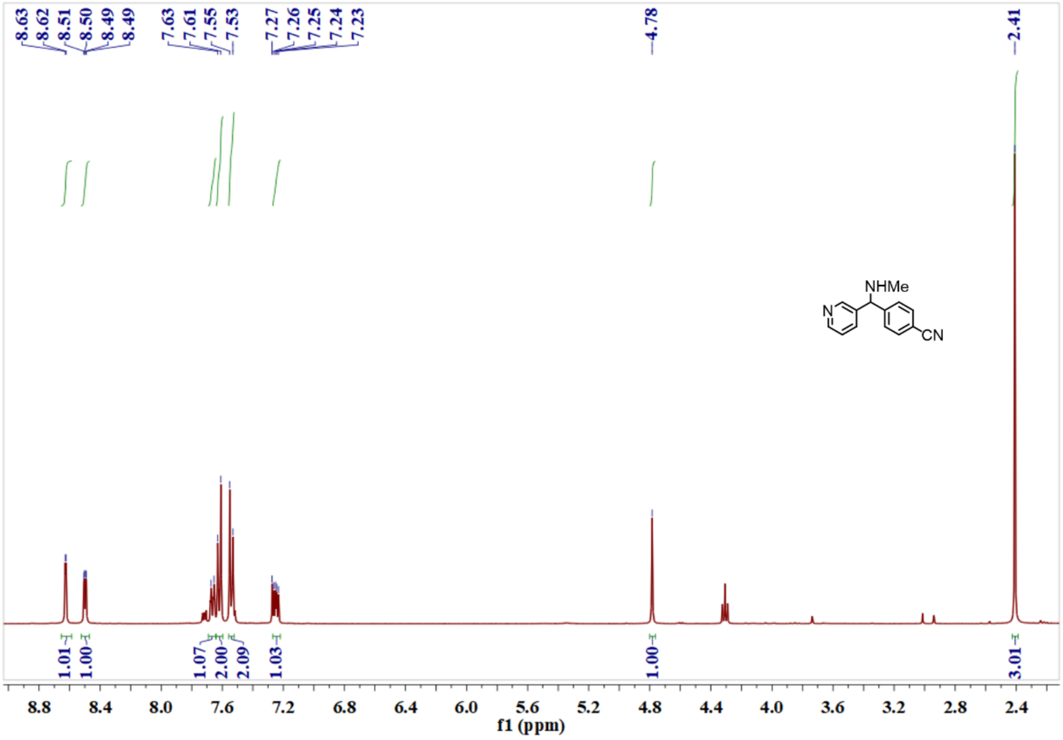

^{1}H NMR (400 MHz, CDCl$_3$-d$_1$) spectrum of 1f

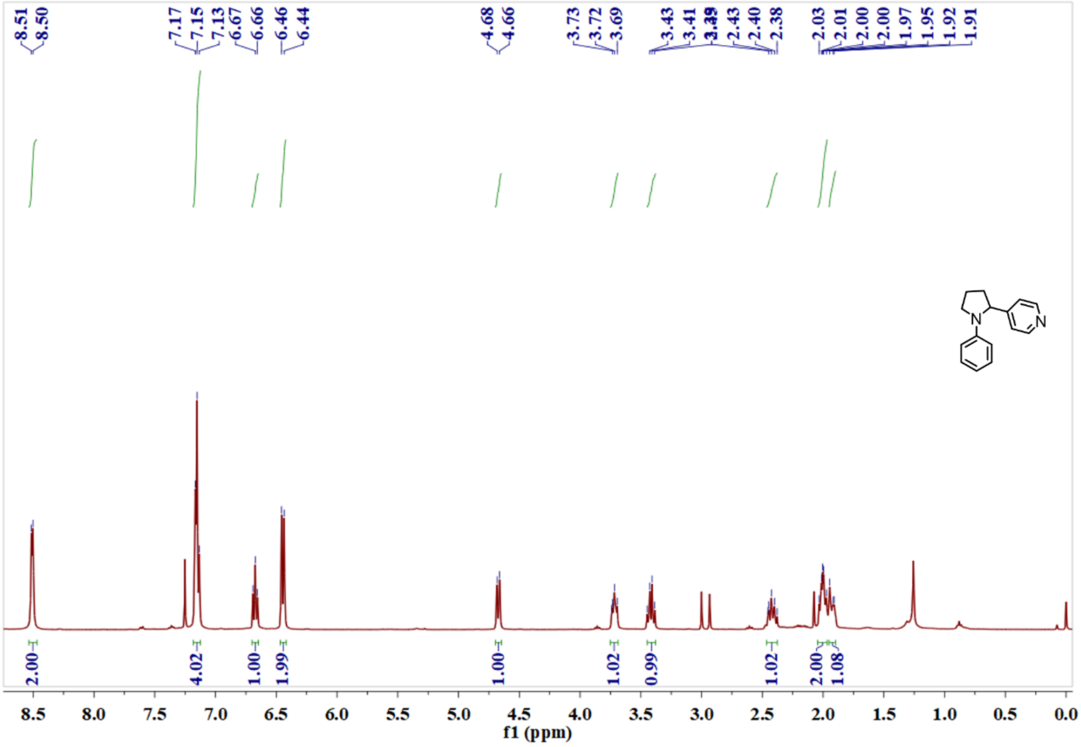

^{1}H NMR (400 MHz, CDCl$_3$-d$_1$) spectrum of 2f

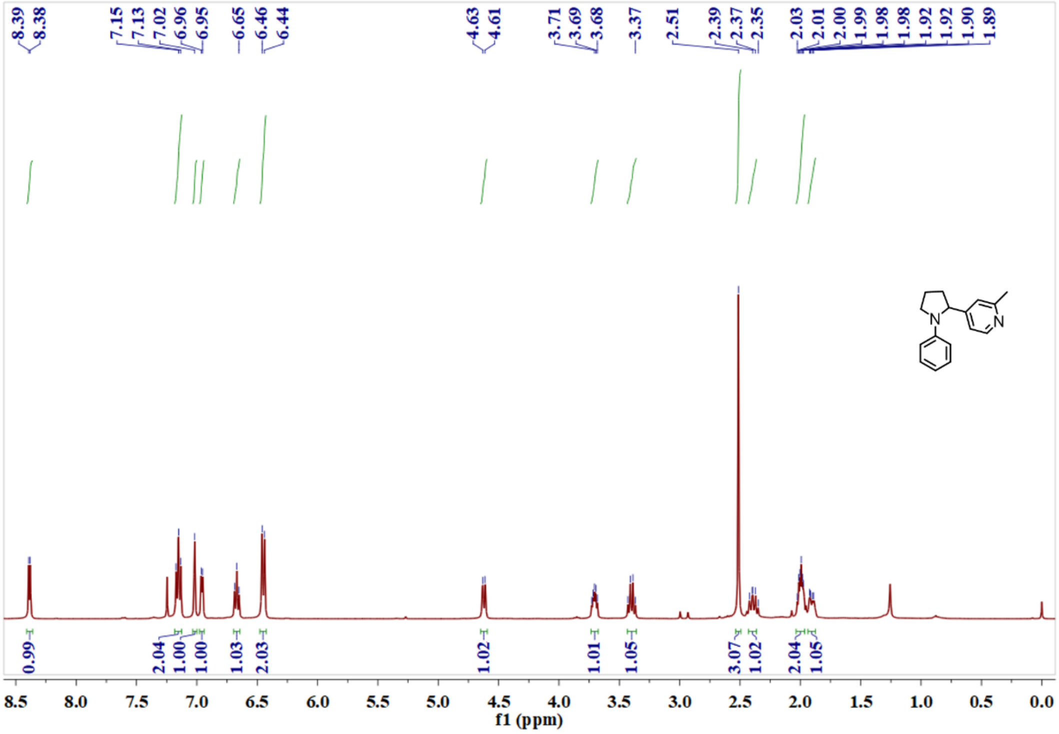

^{1}H NMR (400 MHz, $CDCl_3$-d_1) spectrum of 3f

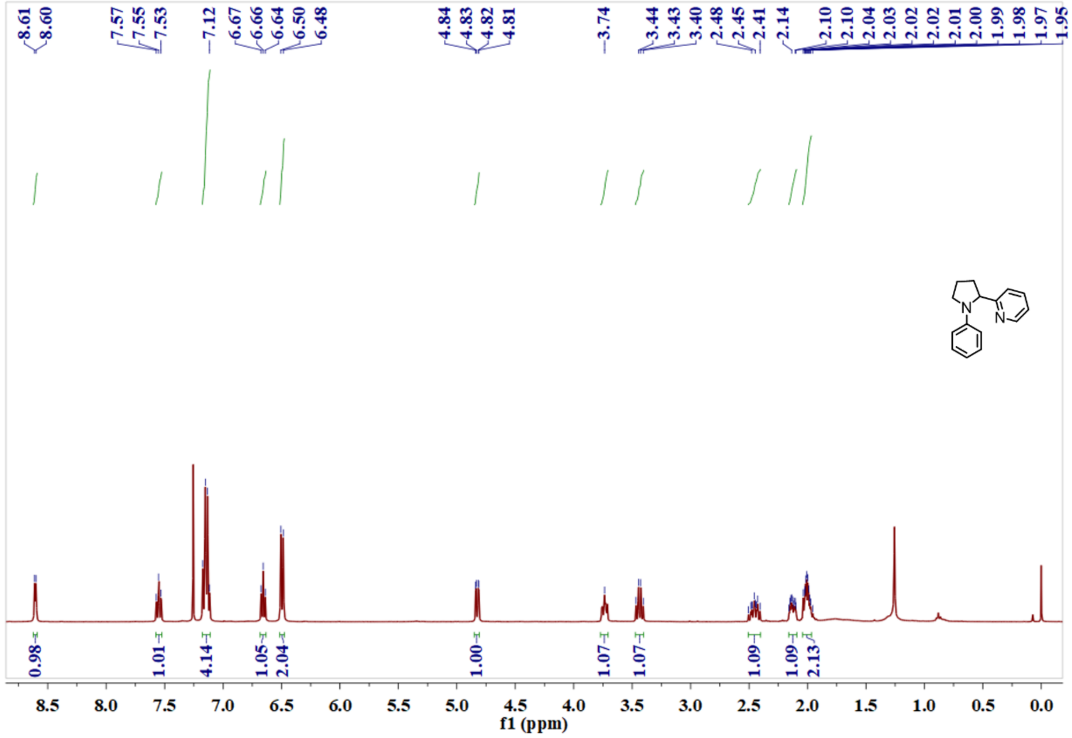

^{1}H NMR (400 MHz, $CDCl_3$-d_1) spectrum of 4f

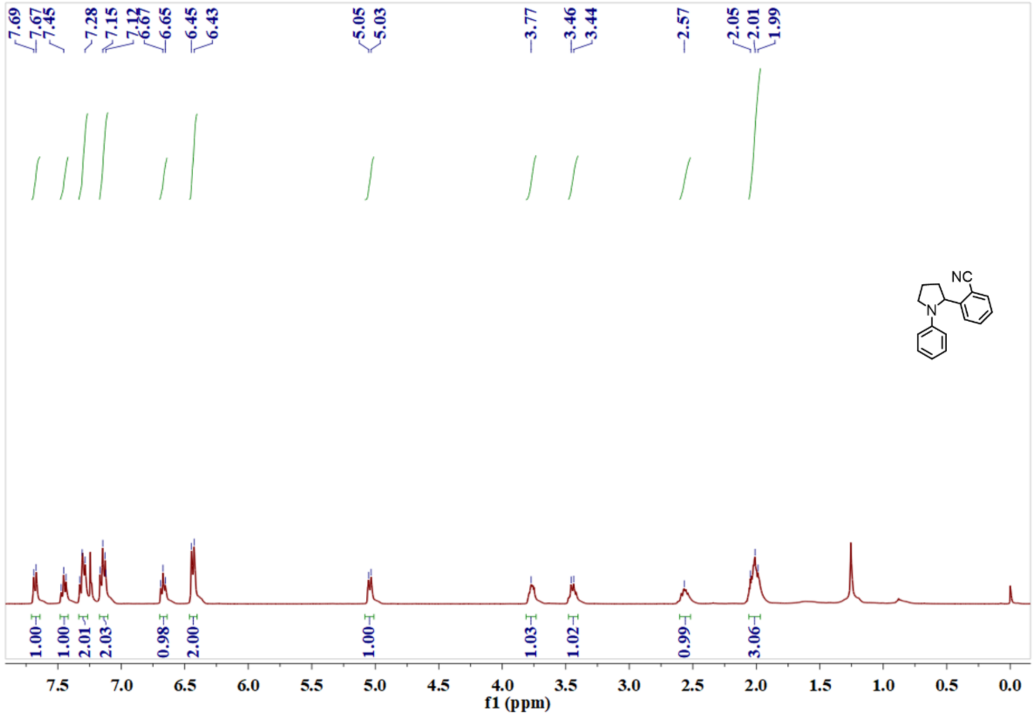

^{1}H NMR (400 MHz, $CDCl_3$-d_1) spectrum of 5f

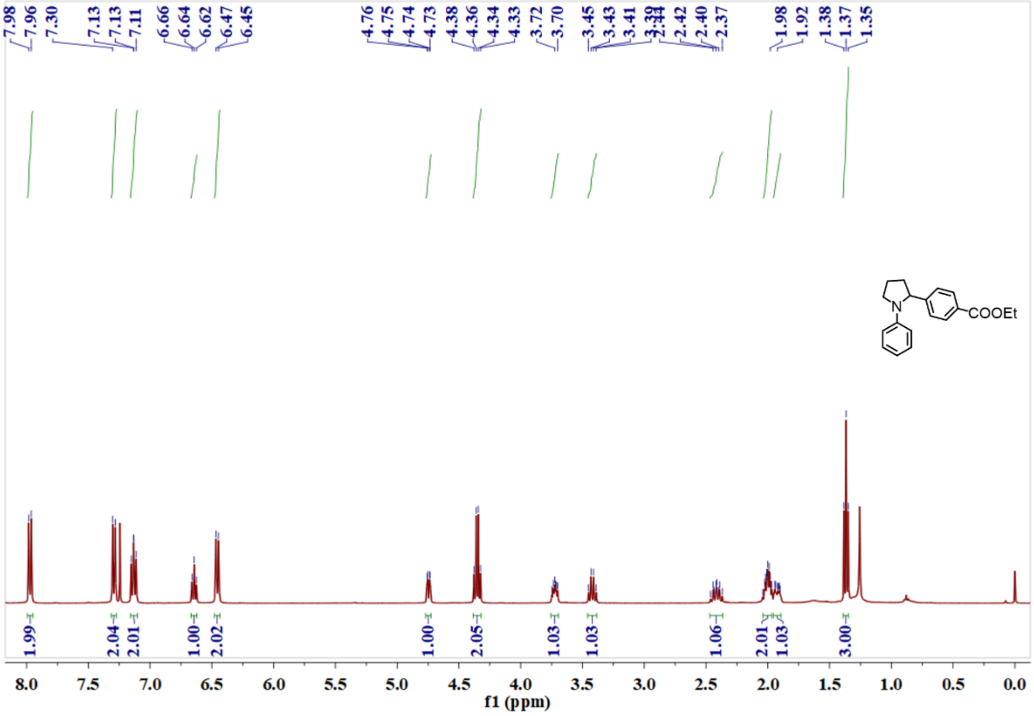

^{1}H NMR (400 MHz, $CDCl_3$-d_1) spectrum of 1g

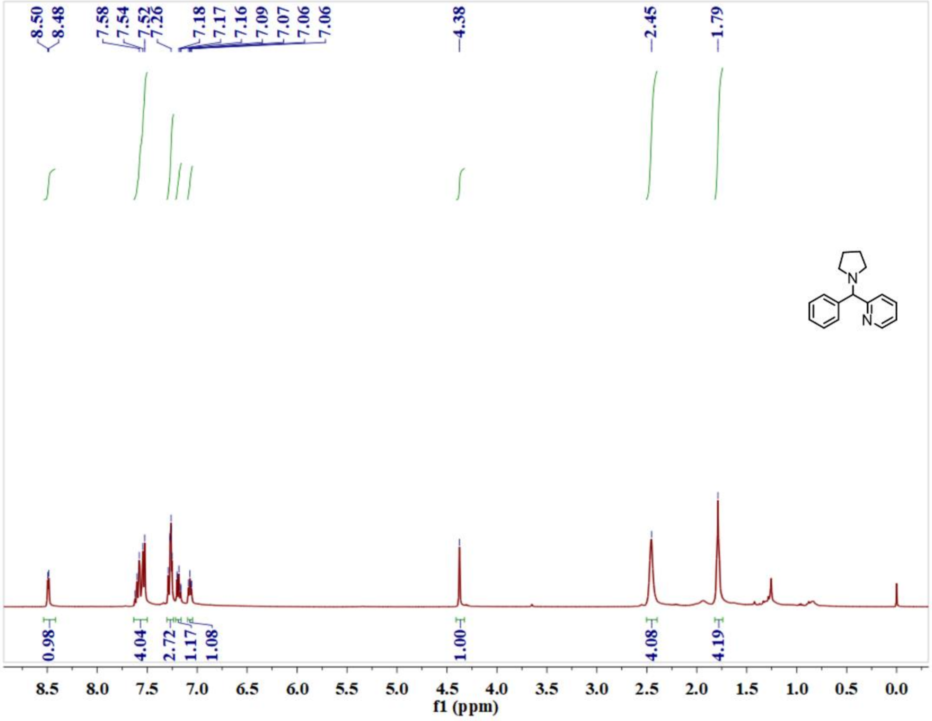

^{13}C NMR (100 MHz, CDCl$_3$-d$_1$) spectrum of 1g

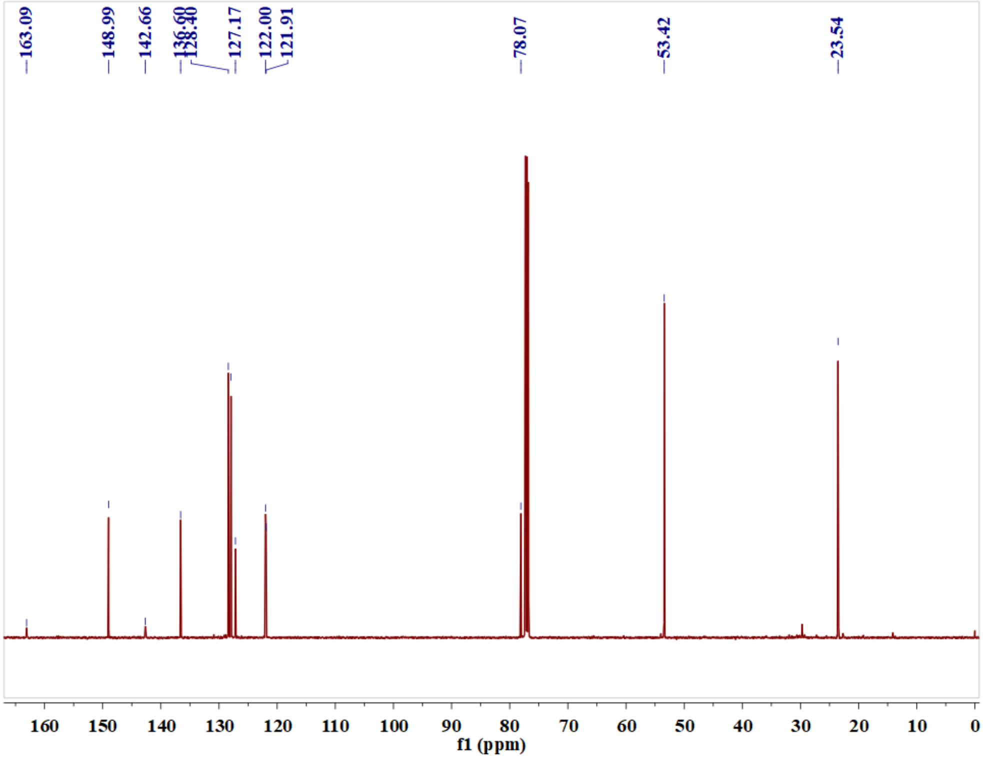

ESI-MS spectrum of 1g

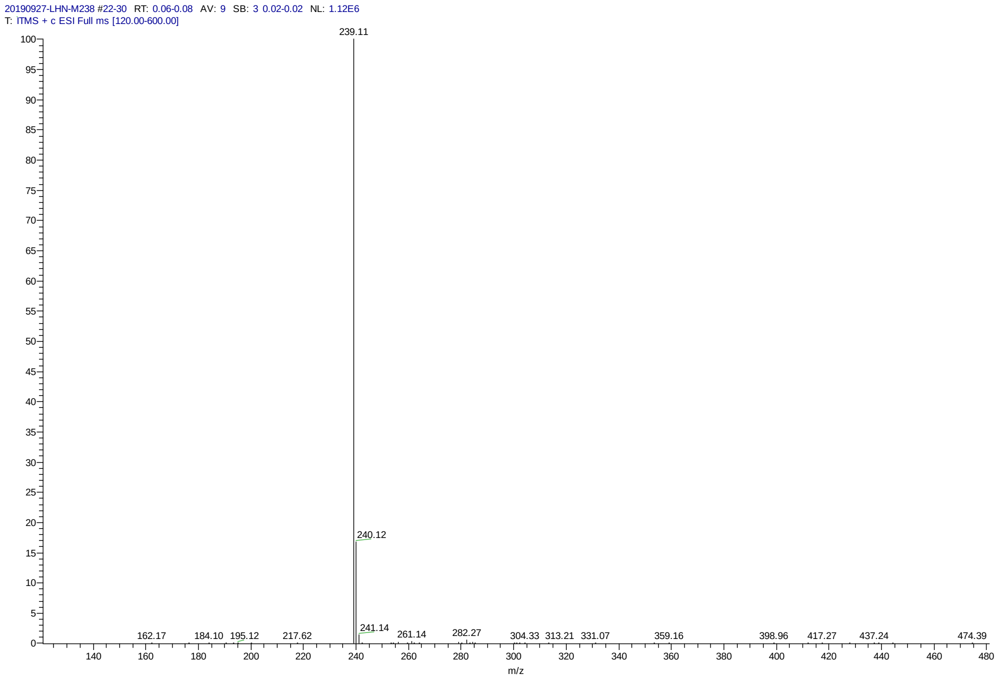

^{1}H NMR (400 MHz, $CDCl_3$-d_1) spectrum of 2g

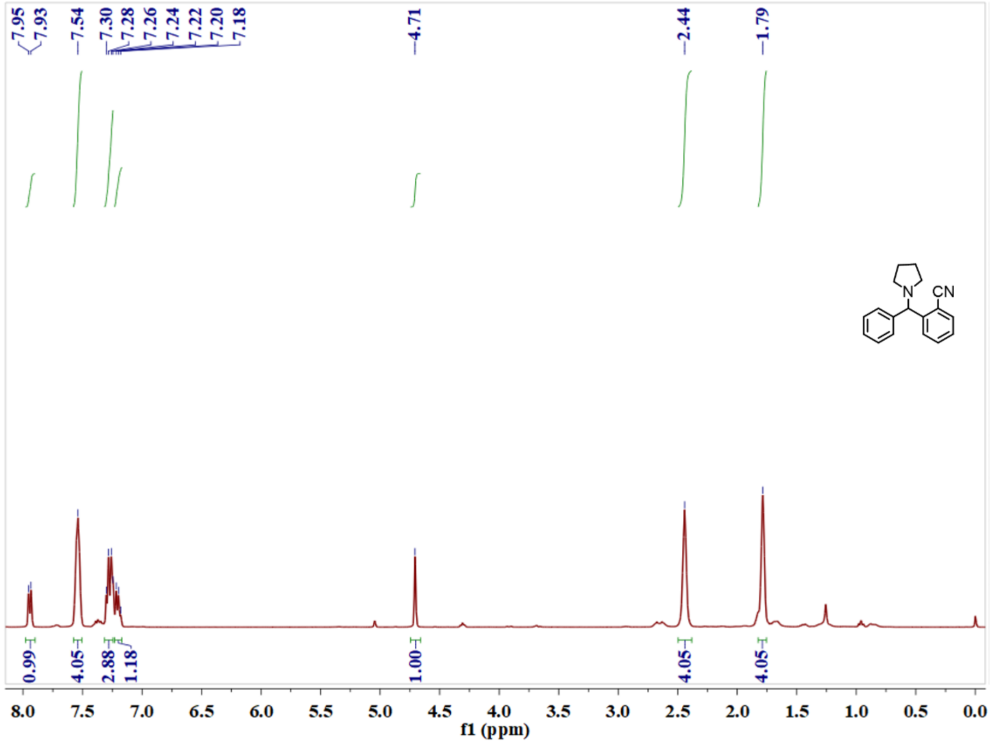

^{13}C NMR (100 MHz, $CDCl_3$-d_1) spectrum of 2g

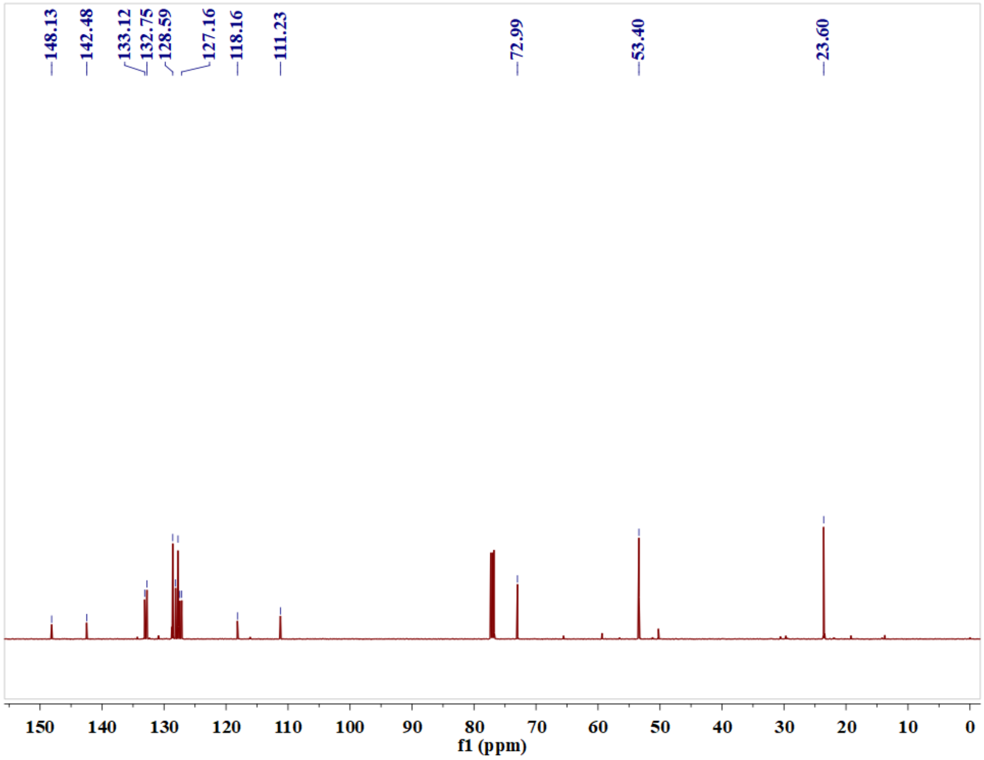

ESI-MS spectrum of 2g

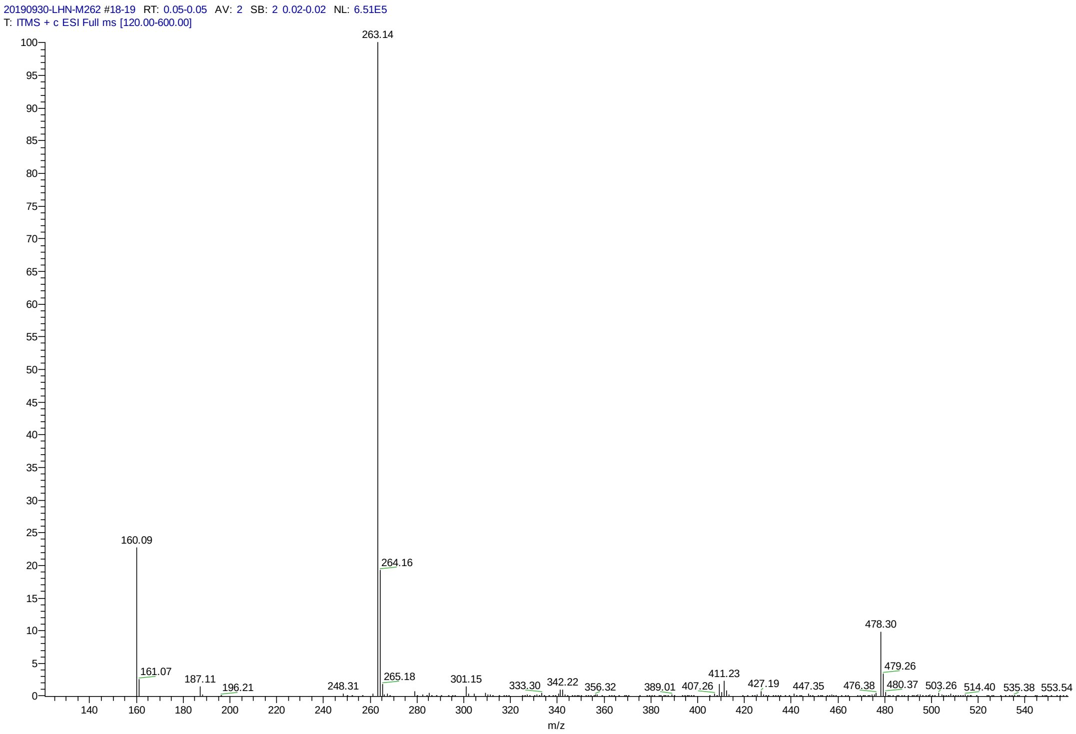

^{1}H NMR (400 MHz, CDCl$_3$-d$_1$) spectrum of 3g

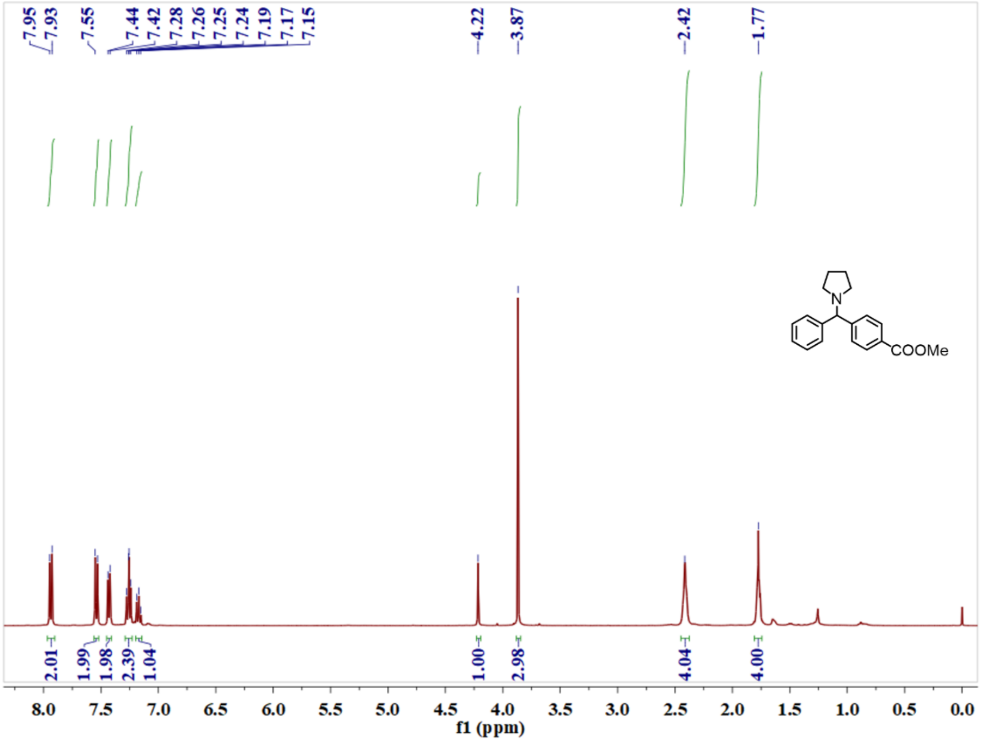

^{13}C NMR (100 MHz, CDCl$_3$-d$_1$) spectrum of 3g

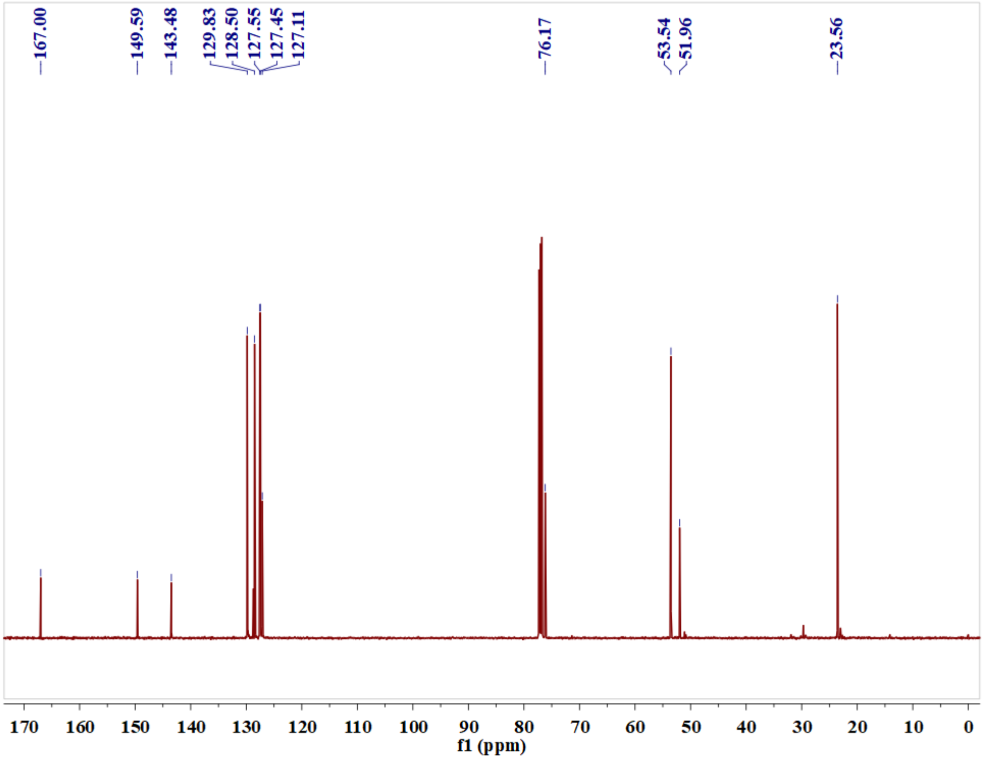

ESI-MS spectrum of 3g

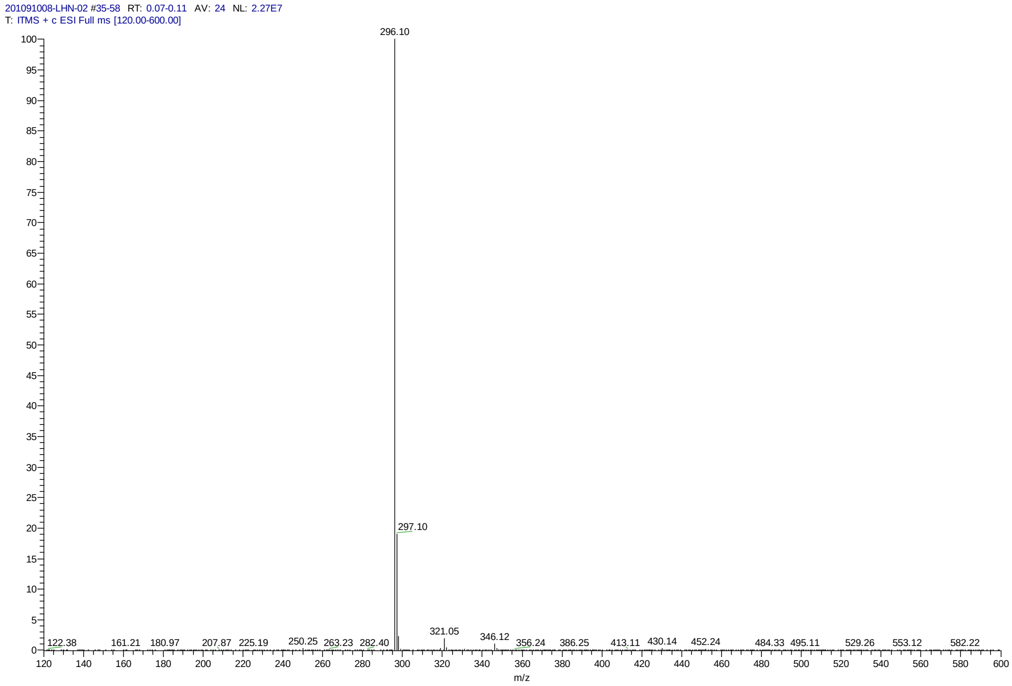

^{1}H NMR (400 MHz, CDCl$_3$-d$_1$) spectrum of 4g

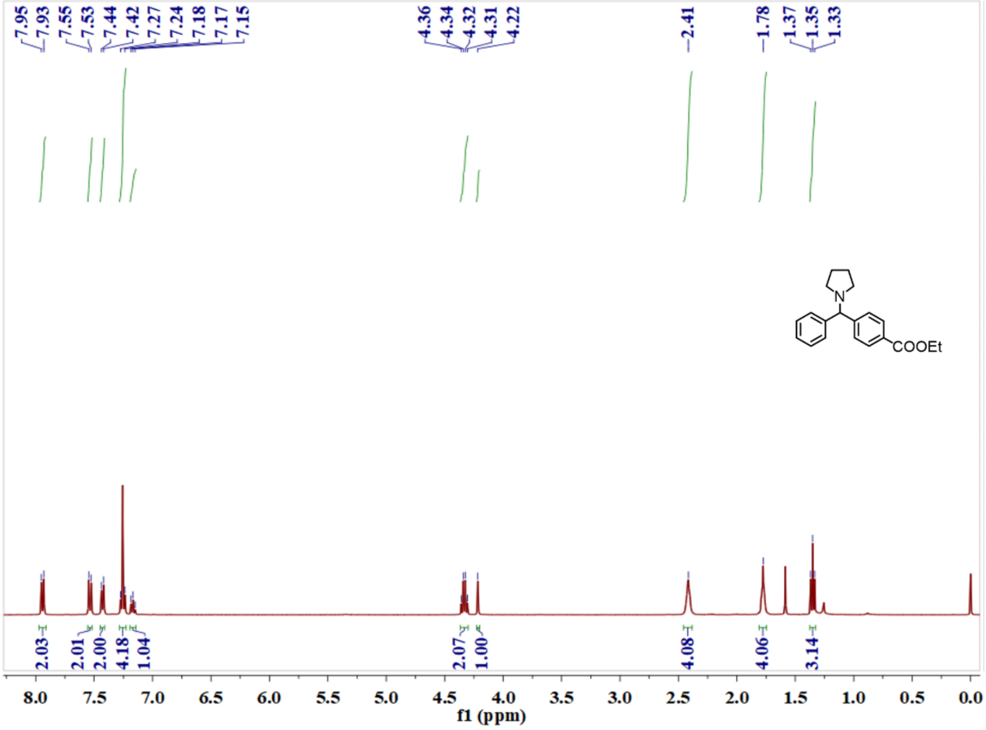

^{13}C NMR (100 MHz, CDCl$_3$-d$_1$) spectrum of 4g

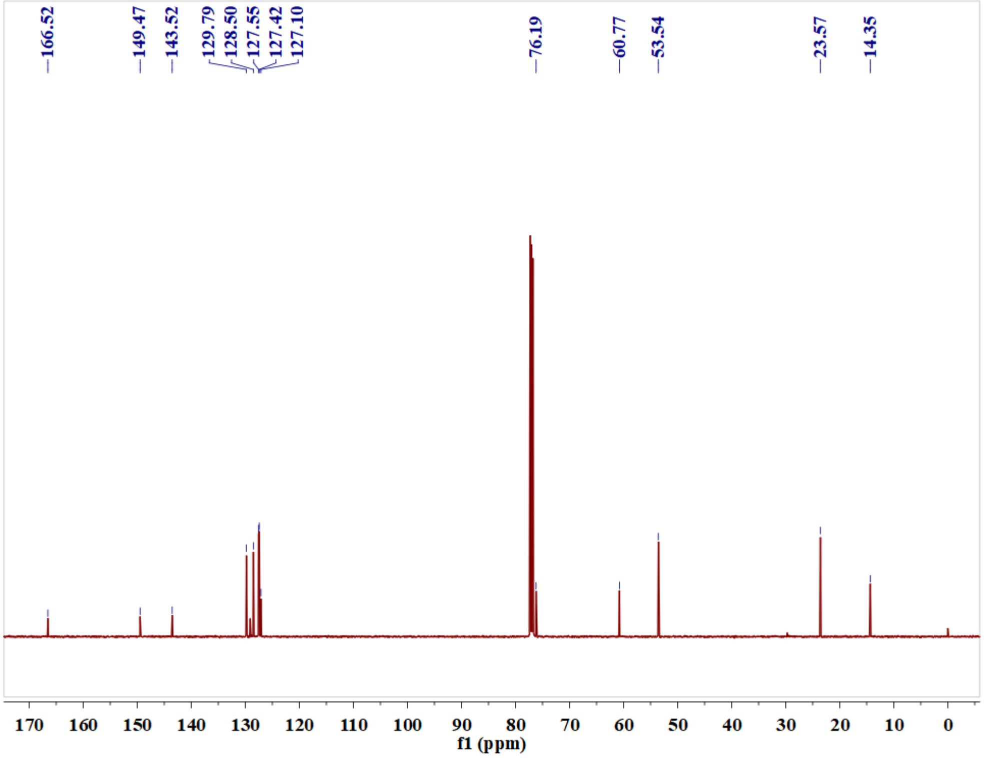

ESI-MS spectrum of 4g